**NASA CONTRACTOR
REPORT**

NASA CR-2022

DEVELOPMENT OF A CATEGORY II APPROACH SYSTEM MODEL

by Walter A. Johnson and Duane T. McRuer

Prepared by
SYSTEMS TECHNOLOGY, INC.
Hawthorne, Calif. 90250
for Ames Research Center

NATIONAL AERONAUTICS AND SPACE ADMINISTRATION • WASHINGTON, D. C. • MAY 1972

1. Report No. NASA CR-2022	2. Government Accession No.	3. Recipient's Catalog No.
4. Title and Subtitle "Development of a Category II Approach System Model"		5. Report Date May 1972
		6. Performing Organization Code
7. Author(s) Walter A. Johnson and Duane T. McRuer		8. Performing Organization Report No. TR 182-2
		10. Work Unit No.
9. Performing Organization Name and Address Systems Technology, Inc. Hawthorne, California		11. Contract or Grant No. NAS 2-4892
		13. Type of Report and Period Covered Contractor Report
12. Sponsoring Agency Name and Address National Aeronautics & Space Administration Washington, D.C. 20546		14. Sponsoring Agency Code

15. Supplementary Notes

16. Abstract

An analytical model is presented which provides, as its primary output, the probability of a successful Category II approach. Typical applications are included using several example systems (manual and automatic) which are subjected to random gusts and deterministic wind shear.

The primary purpose of the approach system model is to establish a structure containing the system elements, command inputs, disturbances, and their interactions in an analytical framework so that the relative effects of changes in the various system elements on precision of control and available margins of safety can be estimated. The model is intended to provide insight for the design and integration of suitable autopilot, display, and navigation elements; and to assess the interaction of such elements with the pilot/copilot.

17. Key Words (Suggested by Author(s)) Category II, approach, aircraft, autopilot, display, model, manual, automatic, wind	18. Distribution Statement UNCLASSIFIED-UNLIMITED		
19. Security Classif. (of this report) UNCLASSIFIED	20. Security Classif. (of this page) UNCLASSIFIED	21. No. of Pages 91	22. Price* 3.00

*For sale by the National Technical Information Service, Springfield, Virginia 22151

FOREWORD

CONTENTS

TABLES

FIGURES

SECTION I

INTRODUCTION

This report documents the development of a low-level approach system model, as one aspect of a terminal area system model, and includes an example of its application. The emphasis is on point of view, technique, and simplicity. As such, the report takes on the characteristics of a tutorial presentation.

A. PURPOSE

The primary purpose of a terminal area system model is to establish a structure containing the system elements, command inputs, disturbances, and their interactions in an analytical framework so that the relative effects of changes in the various system elements on precision of control, pilot/copilot workloads, and available margins of safety throughout the terminal operations envelope can be estimated. It is intended that any such model will be used to provide insight for the design and integration of suitable autopilot, display, and navigation elements; and to assess the interaction of such elements with the pilot/copilot, with emphasis on the automatic/human interfaces.

The model presented herein is an analytical one, and thus has numerical measures of performance as outputs. These outputs include the performance of both human and inanimate components, as well as of the system as a whole. Thus, the model is expected to be extremely useful in:

1. Identifying those system areas which offer the largest immediate possibilities for improvements in safety of operations (and those that offer very little possibility for improvement).

2. Quantifying the prediction of relative performance and safety (or success) margins for competing system (and subsystem) alternatives.

3. Identifying needed research to (a) fulfill a system need, or (b) improve the accuracy of the model.

1

4. Providing a long-range potential, when the model is verified, for computing absolute performance and safety limits (as opposed to relative levels among competing systems) to serve as a guide to the specification of subsystem requirements and as a means for estimating operational statistics.

B. POINT OF VIEW

A logical starting point for presenting the model is to define the desired outputs. Because the approach and landing phases of flight are the most critical, these phases were selected for analysis. This decision led to the desired outputs being the "Basic Outcomes" shown in Table I. In the table the Basic Outcomes are listed together with their "Associated Performance Measures" and "Performance Metrics" (which are computed from the dynamic portions of the system model). A key point in the model is that "Outcome Probabilities" can be computed by combining the critical limits on the performance measures with the values of the performance metrics. Although these probabilities will be only rough approximations for the first-cut model, they will be useful as gross indices and will allow valid comparisons among alternative systems.

As noted in Table I, accidents are very unlikely events, and therefore all accident probabilities are extremely small. Consequently, from a practical standpoint, it is almost a necessity to consider the probability of a missed approach as a primary measure of system adequacy. This point of view is supported by existing information indicating that, at the Category II-B level (see Table II), the missed approach rate can be as high as 40 percent (Ref. 1). In this report we have adopted the FAA position concerning missed approaches (Ref. 11). This is that an approach can be continued below the decision height* (assuming the pilot can see to land) only if the airplane is within 12 ft vertically from the center of the glide slope beam, within 72 ft laterally from the center of the localizer beam, and within 5 kts of the nominal approach

---

*See Table II for a definition of decision height.

2

TABLE I

CONSIDERATIONS FOR APPROACH AND LANDING OUTCOMES

BASIC OUTCOME	ASSOCIATED PERFORMANCE MEASURES	PERFORMANCE METRICS	CRITICAL LIMITS (To achieve outcome)	OUTCOME PROBABILITIES (These are functions of performance metrics and critical limits)	COMMENTS
Successful Landing	Dispersions at decision height and/or reference position and at touchdown	$\mu_h, \sigma_h, \mu_y, \sigma_y, \mu_u, \sigma_u, \mu_E, \sigma_E$	Airplane must be within successful-landing "window"	P_{OK}	Because successful landings and missed approaches will account for almost all approaches, P_{MA} will be a very significant parameter. $(P_{OK} \doteq 1 - P_{MA})$
Successful missed approach	Dispersions at decision height	$\mu_h, \sigma_h, \mu_y, \sigma_y, \mu_u, \sigma_u, \mu_E, \sigma_E$	Airplane must be outside of successful approach window but within successful "go-around" window	P_{MA}	
Short landing	Longitudinal touchdown location	$\mu_{x_{TD}}, \sigma_{x_{TD}}$	$x_{TD} < x_{TD_{MIN}}$	P_{SL}	The sum of the various accident probabilities will be considerably smaller than P_{MA}. (The sum should be of the order of 10^{-6} or smaller.)
Hard landing	Sink rate at touchdown	$\mu_{\dot h_{TD}}, \sigma_{\dot h_{TD}}$	$|\dot h_{TD}| > |\dot h_{TD}|_{MAX}$	P_{HL}	
Overrun runway during rollout	Airspeed and altitude errors at reference position	μ_E, σ_E	$\underbrace{K_1 \Delta h_R + K_2 \Delta u_R}_{E} > E_{MAX}$	P_{OR}	
Land off side of runway	Lateral touchdown location	$\mu_{y_{TD}}, \sigma_{y_{TD}}$	$|y_{TD}| > y_{TD_{MAX}}$	P_{LO}	
Drag a wing tip or engine pod during landing	Bank angle at touchdown	$\mu_{\phi_{TD}}, \sigma_{\phi_{TD}}$	$|\phi_{TD}| > \phi_{TD_{MAX}}$	P_{DW}	
Land with excessive misalignment angle (putting side loads on landing gear)	Side velocity at touchdown	$\mu_{v_{TD}}, \sigma_{v_{TD}}$	$|v_{TD}| > v_{TD_{MAX}}$	P_V	
Run off side of runway during rollout	Lateral displacement deviations during rollout	$\mu_{y_{RO}}, \sigma_{y_{RO}}$	$|y_{RO}| > y_{RO_{MAX}}$	P_{RO}	

(Left margin vertical label for rows 3–9: ACCIDENT OR CRASH)

TABLE II

ICAO LOW-VISIBILITY-LANDING ILS CATEGORIES

CATEGORY	RUNWAY VISUAL RANGE (RVR) ft	DECISION HEIGHT (DH)* ft
I	2,400	200
II-A	1,600	150
II-B	1,200	100[†]
III-A	700	—
III-B	150	—
III-C	zero	—

*A height (above runway elevation) below which a pilot must not descend if he has not obtained adequate visual references to land; i.e., he must execute a missed approach at this point if he does not have adequate references to land by visual means.

[†]Sometimes called CAT II.

speed. These limits constitute an effective "window" at the decision height. If the airplane is not within the window, then a missed approach is mandatory. For practical operations, making the Category II-B window a very large proportion of the time, say 95-99 percent, may be the most difficult part of the approach and landing sequence. However, once this window is made, only the flare and removal of crab or wing-down are required to get on the ground with reasonable touchdown conditions. Therefore, the occurrence of short landings and off-runway landings should decrease when using the Category II window (while most of the other outcome probabilities would be expected to be fairly similar to current operational experience). In any event, for a first-cut evaluation, we will direct most of our calculations to considerations of successful approaches and missed approaches. This will in no way detract from the generality of the technique, but will greatly simplify the mathematics involved. Hence, a much more straightforward presentation is possible.

C. OVERVIEW OF ANALYSIS

To estimate the performance metrics and outcome probabilities requires a dynamic model and probability performance trees (among other things). An overview of the various analysis steps is provided in Fig. 1. The dynamic model is made up of blocks 1 to 4. The results of these first blocks are, in essence, feedback control systems which satisfy the guidance and control requirements for approach and landing. The airplane is the controlled element and the active elements of the feedback controller may be either the pilot, autopilot, or a split-axis pilot/autopilot combination. In addition, the systems contain passive or monitoring elements: the copilot, for the manual control situation, or the pilot and copilot for the automatic condition. The system mechanizations (Block 2) can be made appropriate for:

- Fully automatic approach and landing
- Flight director plus pilot/vehicle approach and landing
- VFR pilot/vehicle approach

The first two system mechanization possibilities are representative of advanced low-visibility approach and landing systems. The last one is still semiconjectural in that a scanning multiloop pilot model has not yet been validated for such a complex situation.

Exercise of the dynamic model with the inputs and disturbances selected in Block 4 provides the performance metrics of Table I. Conventionally, this block, noted as 7 on Fig. 1, would use ordinary aircraft motions and kinematic quantities as the dependent variables. However, in some cases we have found it possible to select combinations of these variables as composite "state" variables which are more directly related to the basic outcomes (such as runway overruns) than are the standard aircraft motion quantities. Consequently these state variables are used, where appropriate, as part of the basic dynamic model to ease the transition between performance metrics and the ultimate outcome probabilities. With the composite state variables included, the
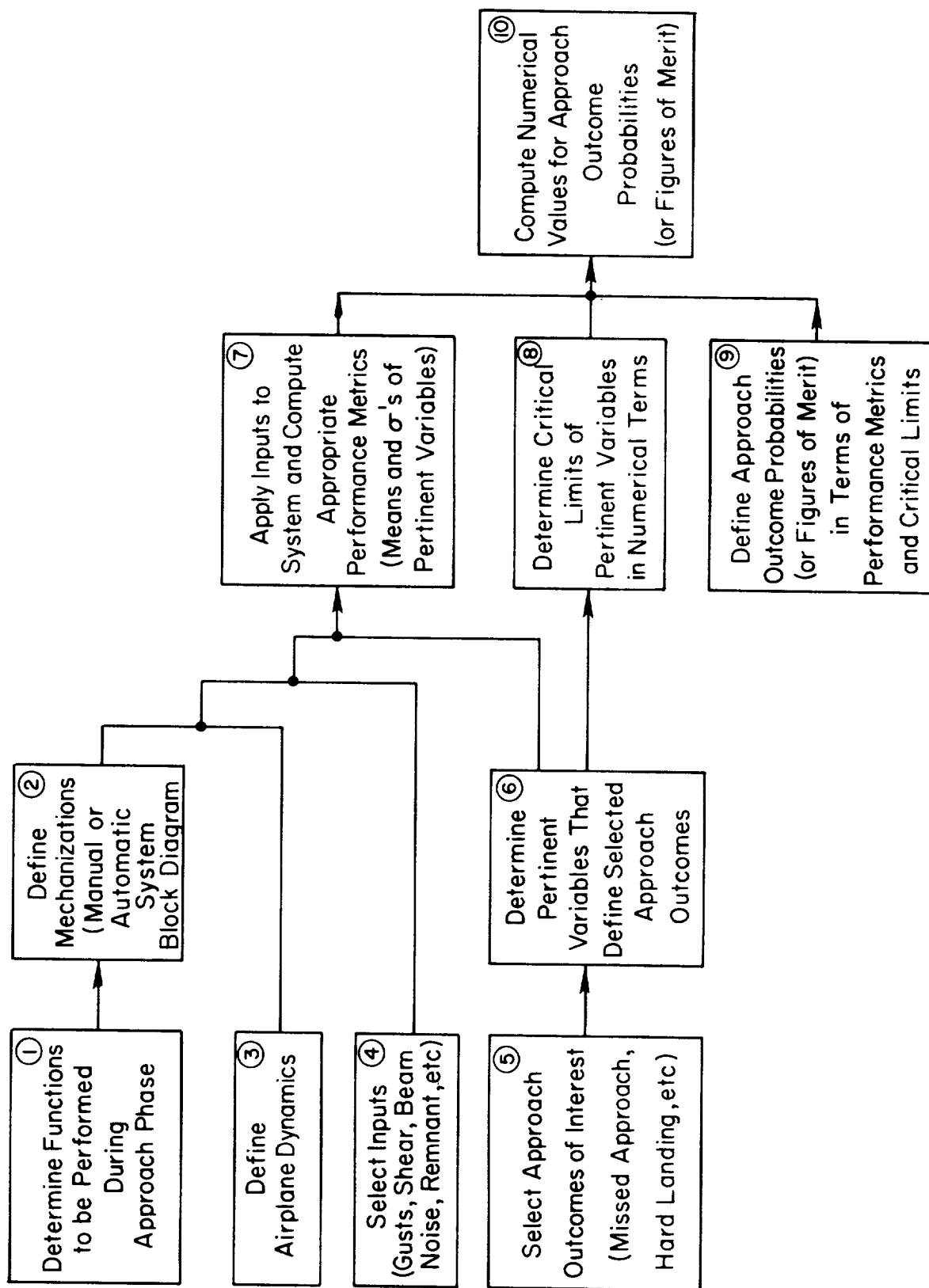
Figure 1. Overview of Analysis Steps Leading to Evaluation of Category II Approach and Landing Systems

The flow chart contains the following boxes:

① Determine Functions to be Performed During Approach Phase

② Define Mechanizations (Manual or Automatic System Block Diagram)

③ Define Airplane Dynamics

④ Select Inputs (Gusts, Shear, Beam Noise, Remnant, etc)

⑤ Select Approach Outcomes of Interest (Missed Approach, Hard Landing, etc)

⑥ Determine Pertinent Variables That Define Selected Approach Outcomes

⑦ Apply Inputs to System and Compute Appropriate Performance Metrics (Means and σ's of Pertinent Variables)

⑧ Determine Critical Limits of Pertinent Variables in Numerical Terms

⑨ Define Approach Outcome Probabilities (or Figures of Merit) in Terms of Performance Metrics and Critical Limits

⑩ Compute Numerical Values for Approach Outcome Probabilities (or Figures of Merit)

6

"extended" dynamic model then comprises Blocks 1 through 6, with Block 7 being its actual exercise for a particular system and set of conditions.

With the performance metrics available, and critical limits and approach outcome probabilities defined (Blocks 8 and 9 in Fig. 1), the numerical values for the approach outcome probabilities can be computed (Block 10). The result is then a set of performance metrics and outcome probabilities for a specific system mechanization subjected to a given input and disturbance environment. Direct comparisons of automatic systems can be made simply by going through these analysis steps for each competing system mechanization with a standardized set of inputs. It is noted that the role of incorrect pilot decisions for the execution of missed approaches is not considered here. Such a refinement is left to future versions of the model.

In this report the intention is to develop and describe the model as outlined above.

D. OUTLINE OF THE REPORT

Using the framework from the above overview, Sections II through V present the information called for in the various blocks of Fig. 1. Section VI then follows with a summary and some conclusions. Peripheral material is found in the appendices and in Ref. 12.

SECTION II

DESCRIPTION OF FUNCTIONS TO BE PERFORMED DURING APPROACH

During the approach phase of flight there are a large number of tasks
to be performed (and monitored) by the flight crew. These tasks include
going through checklists, tuning radios, carrying on communications with
controllers on the ground, navigating per ATC clearances, etc., as well
as flying the airplane. A list of these tasks, when they should be per-
formed, and the associated numerical parameters are given in Fig. 2. In
addition to this overall view of the approach situation, Fig. 3 has a
detailed view of the situation in the vicinity of the airport.

For our purposes, the tasks of primary interest are glide slope and
localizer tracking from the outer marker to the decision height. These
tasks can be performed automatically (with an autopilot), manually (with
a flight director), or via a combination of automatic and manual control.
In this report we will consider the functions which must be accomplished
by any form of control, and shall illustrate their actual performance both
with fully automatic equipment and a manually controlled flight director.
Modifications made to the analytical details to make them suitable for
manual control are described in Appendix B.[*] In the initial system analy-
ses no autothrottle or speed control is considered. Thus the basic system
is evaluated first, and the effects of system perturbations can be assessed
later. A detailed discussion of the functional requirements of the control
system and the means for satisfying the requirements is presented in Ref. 12.

Although only the primary tasks of glide slope and localizer tracking
are considered herein, such secondary tasks as system monitoring and fault
detection are recognized as being equally important for achieving a success-
ful approach. However, analysis of these aspects of system operation is
beyond the scope of this initial system modelling.

---

[*]Briefly, the major modifications required to cover manual control are
the addition of pilot lags in responding to displayed errors, and the intro-
duction of pilot-generated remnant into the elevator, aileron, etc., com-
mands. The amount of remnant is determined by the displays used and the
associated scanning required to close the various loops.

PHASE OF FLIGHT	LOCATION ON FIGURE	EVENT	REFERENCE	REMARKS
Preliminary preparations for approach	A	Complete preliminary before-landing checklist. Check that all systems are intact and operating (no flags). Tune and identify 2 VHF radios to localizer frequency. Tune and identify 2 ADF's to LOM (LMM). Set marker beacon switches and test. Set decision height on radio altimeter. Set inbound ILS localizer heading on respective course indicators	10-30 miles from airport. OM high sensitivity, MM low sensitivity, 100 ft for Category II	Includes autopilot and flight director annunciator system
Initiation of lateral guidance acquisition	B	Maneuver airplane to acquire heading that will intercept localizer beyond outer marker at an angle of less than 90°. If intercept angle is greater than 90° then select the heading that will take airplane over outer marker (where a procedure turn will be made)	10-30 miles from airport	Intersect localizer at least 3 miles beyond outer marker
Preparations for acquiring vertical guidance	C	Acquire initial approach airspeed and partial flaps	V_{ref} + 30 kt, 20°	V_{ref} = 1.3 V_{stall} full flaps (= bug speed)
	D-E	Descend to (and maintain) initial approach altitude	≈ 1500 ft above field elevation	
	E	Set speed command system to desired speed and engage autothrottle. Increase flaps and reduce speed.	V_{ref} + 20 kt, 30°	
Acquisition of lateral guidance	F	Initiate capture of localizer beam	At least 3 miles from outer marker	
	G-J	Stabilize on lateral flight path	Prior to outer marker	
	G-Q	Maintain lateral guidance		Beam width is ±2-1/2° from beam center
Acquisition of vertical guidance and completion of preparations for landing	H	Lower landing gear when glide slope needle becomes "alive"		
	I	As G/S needle reaches one dot "fly up", lower more flaps and start bleeding more airspeed.	40°, V_{ref} + 10 kt	
	J	Capture glide slope beam — extend flaps 100%, acquire final approach airspeed, and establish sink rate. With safe landing gear indication, complete "Final checklist"	50°, V_{ref} + 5 kt, Sink rate ≈ 700 FPM	Intercept G/s bullseye and pitch over to follow beam
	J-K	Stabilize on vertical flight path	Within 2 miles from outer marker	
	J-M	Maintain vertical guidance		Beam width is ±0.7° from beam center. Errors should not exceed one dot. Constant sink rate is desired.
Final approach	K-M	Airplane stabilized on flight path in all axes	Still more than 500' ft above terrain	For Category I — execute missed approach if field not in sight.
Glide slope extension	L-M	Use extended glide slope or Category II beam for vertical guidance	Middle marker is at Category I decision height (200 ft)	For Category II — continue to 100 ft decision height
Flare	M-P	Reduce sink rate	From ≈ 11 ft/sec to ≈ 2 ft/sec	Reduce airspeed gradually during flare. Flare begins at about 40 ft altitude.
	N-P	Decrab to align airplane with runway	At ≈ 12 ft	If decrab at higher altitude, can use forward slip until ≈ 10 ft and then level wings for touchdown.
Touchdown and rollout	P	Contact with ground	Within 2,000 ft from threshold	
	P-Q	Airplane decelerates to a stop		

Figure 2. Tasks Performed during Approach and Landing

9
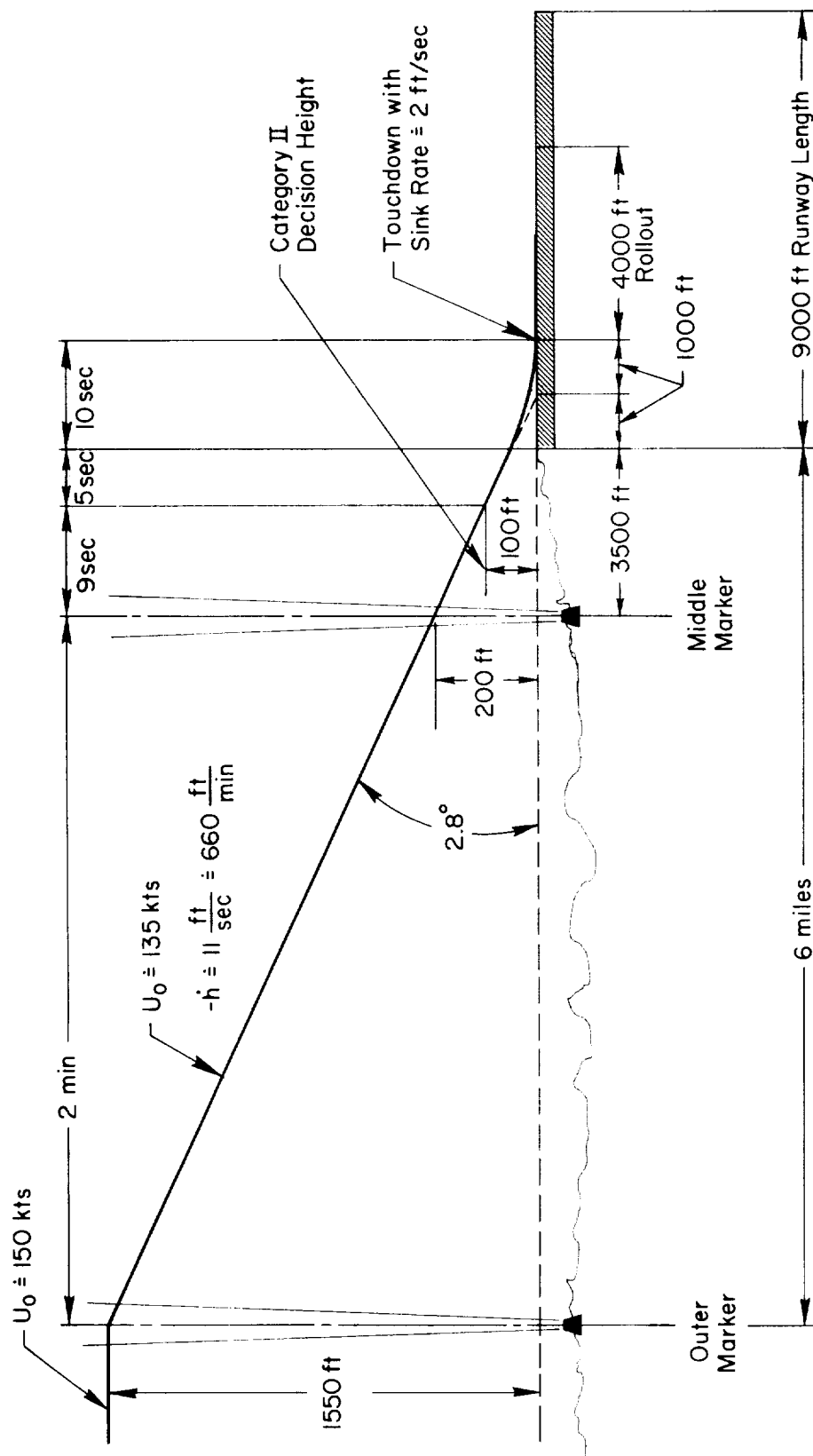
Figure 3. Typical Numbers Associated with an ILS Approach and Landing

10

SECTION III

SYSTEM INPUTS

For the purposes of evaluating and comparing systems it is necessary to subject them to an appropriate set of inputs. To cover a variety of situations, three types of input disturbances which are commonly encountered during an approach were considered.

- Random gusts
- Deterministic gusts
- ILS beam noise

They shall be described in this same order below, and then summarized in a table at the end of this section.

A. RANDOM GUSTS

The random gusts considered here are defined by components along all three axes. Since analysis of measured gust data has revealed nearly Gaussian distributions, the assumption of zero-mean Gaussian distributions for random gusts appears to be justified.

Considerable gust data from numerous sources have been integrated to produce a gust model appropriate for design analysis purposes. The pertinent aspects of this model are given in Ref. 2. The Dryden form of the model was selected for ease of computation. The basic form of the model is defined by three power spectral densities which relate normalized gust intensities to spatial "frequency." In terms of temporal frequency these spectra are given by

$$\Phi_{u_g}(\omega) = \sigma_{u_g}^2 \frac{2L_u}{\pi U_0} \frac{1}{1 + \left(\frac{L_u \omega}{U_0}\right)^2} \tag{1}$$

$$\Phi_{v_g}(\omega) = \sigma_{v_g}^2 \frac{L_v}{\pi U_0} \frac{1 + 3\left(\frac{L_v \omega}{U_0}\right)^2}{\left[1 + \left(\frac{L_v \omega}{U_0}\right)^2\right]^2} \tag{2}$$

$$\Phi_{w_g}(\omega) = \sigma_{w_g}^2 \frac{L_w}{\pi U_0} \frac{1 + 3\left(\frac{L_w \omega}{U_0}\right)^2}{\left[1 + \left(\frac{L_w \omega}{U_0}\right)^2\right]^2} \tag{3}$$

11

where L_u, L_v, L_w = scale lengths (ft)

U_0 = aircraft's mean speed with respect to the air mass (ft/sec)

ω = frequency (rad/sec)

σ = standard deviation

An additional spectrum of interest is derivable from these basic spectra, and is given by

$$\Phi_{p_g}(\omega) = \left(\frac{\sigma_{w_g}^2}{U_0 L_w}\right) \frac{0.8\left(\frac{\pi L_w}{4b}\right)^{1/3}}{1 + \left(\frac{4b}{\pi U_0}\right)^2} \qquad (4)$$

where b = wing span (ft).

Conforming to the stipulations given in Ref. 2, the random turbulent velocity components have been assumed to be uncorrelated. While this assumption is fully justified for clear air turbulence at high altitudes, it is not strictly true at low altitudes because of prevailing anisotropy in the boundary layer. However, it is also pointed out in Ref. 2 that at low altitudes the cross-correlations between the gust components are weak, and may therefore be disregarded.

In view of the above, it is assumed that the three velocity components, u_g, v_g, and w_g, are mutually uncorrelated, so that analysis can be carried out using the three components of the gust model separately.

The procedure for evaluating the spectra is outlined in the following. It is based on extensive data fitting and adjusting of the Dryden "scales" to make all three scales (L_u, L_v, and L_w) equal at an altitude of 1,750 ft. The resulting scale lengths for clear air turbulence for the above spectral forms are

Below 1,750 ft: $\qquad L_w = h \text{(ft)}$ $\qquad\qquad (5)$

$$L_u = L_v = 145(h)^{1/3} \text{(ft)} \qquad (6)$$

12

The variation of L_u and L_v at low altitudes according to the one-third power of altitude above ground level is simply a mechanism that forces the scales of the two horizontal gust components to be larger than the vertical scale. (Although these formulae produce correct trends, there is little data available that can be used to substantiate the $h^{1/3}$ relationship in L_u and L_v.)

This gust model represents stationary, random gusts as stationary processes. However, the gusts actually <u>encountered</u> by a <u>descending</u> airplane are nonstationary due to the altitude dependence of the gust characteristics. Further, because the break points in the analytic expressions for the gust power spectra are nonlinear functions of altitude, the spectral characteristics of the gusts encountered by a descending airplane are nonlinear functions of time. However, in spite of these complicating factors, reasonably accurate performance calculations can still be made quite simply. This is explained in the following paragraphs.

It is a straightforward calculation to compute the rms output of a linear system to a stationary random input. Figure 4 illustrates this. Implicit in these calculations is the assumption that the system has been operating for a sufficiently long (theoretically infinite) time so that all transients have died out. However, for practical purposes all that is really required is that "steady-state" conditions have been reached, i.e., that the system has been operating on the stationary input long enough for the output to become approximately stationary.

Input   Output
Spectrum   Spectrum

Φ_{ii} Φ_{cc}

$$\Phi_{cc}(\omega) = |G(j\omega)|^2 \, \Phi_{ii}(\omega)$$

G(s)

$$\sigma_c^2 = \int_0^\infty \Phi_{cc}(\omega) d\omega$$

Linear
System
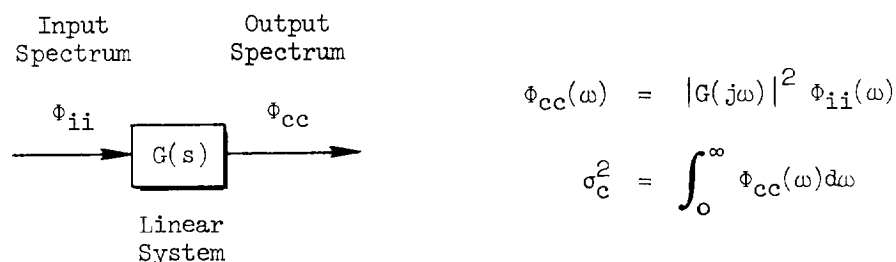
Figure 4. Computation of RMS Output from Input Spectrum
and System Transfer Function

13

The time required for this to occur depends on the system dynamics. For our model airplane plus controller this time is relatively short — of the order of 5 to 10 sec (based on the settling time for step inputs). As an analogous example, Fig. 5 shows a plot from Ref. 3 of σ_h versus time for an F4D-1 tracking a visual glide slope beam during a constant speed approach to an aircraft carrier. For this plot, random beam motion was initiated at t = 0 sec. The plot shows that 80 percent of the steady-state airplane σ_h is reached in 5 sec, and 90 percent in 7-1/2 sec.
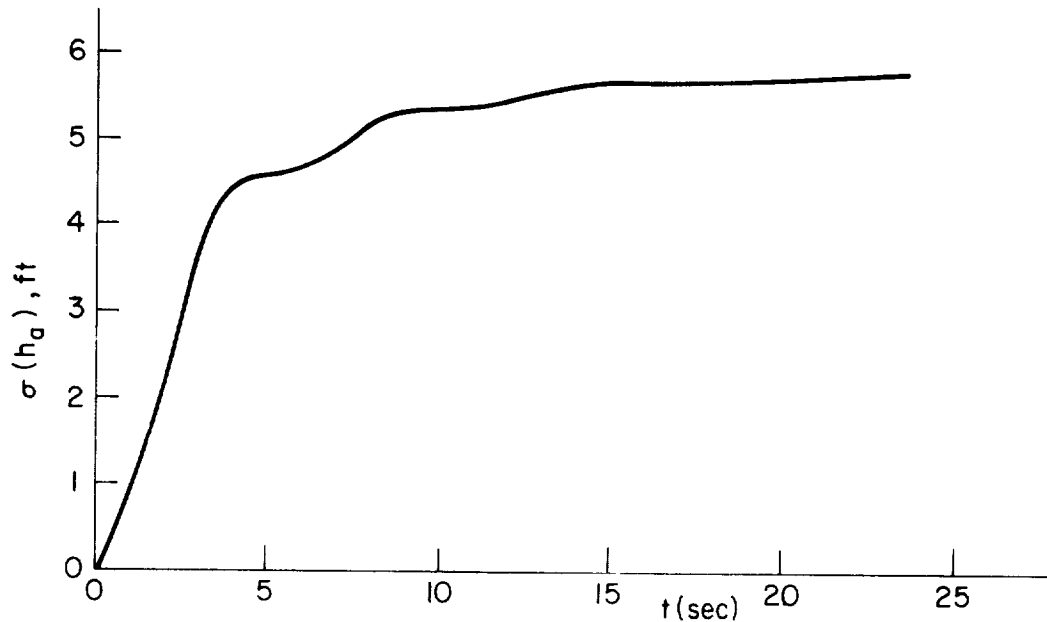
Figure 5. Aircraft Altitude Excursions
Resulting from Pilot's Tracking the Beam

Thus, although the mathematics requires a stationary input to be applied to a system for an infinite time, only the most recent 10 sec (or so) of input has any appreciable effect on the airplane's current condition. This observation has profound consequences, the most pertinent of which is that the complete nonstationary gust input to the descending airplane is not required to estimate the airplane dispersions at the Category II decision height of 100 ft altitude. Instead, only

the gust characteristics corresponding to the last 5-10 sec preceding the altitude of interest need be considered. Because the airplane sink rate is about 10 ft/sec, 5 to 10 sec corresponds to about 50 to 100 ft altitude change. For such a small altitude change the altitude-dependent gust parameters do not change very much during the time interval of interest. Therefore, the required "short-time" gust model is essentially a stationary input which is closely approximated by the gust model components evaluated at an altitude of 100 ft. This yields

$$L_W = 100 \ (\text{ft}) \tag{7}$$

$$L_u = L_v = 145(100)^{1/3} = 673.0 \ (\text{ft}) \tag{8}$$

The gust intensities along the various axes for Dryden form spectra are related by the expression

$$\frac{\sigma_{u_g}^2}{L_u} = \frac{\sigma_{v_g}^2}{L_v} = \frac{\sigma_{w_g}^2}{L_W} \tag{9}$$

Thus, the ratios of σ_{u_g} and σ_{v_g} to σ_{w_g} will be

$$\frac{\sigma_{v_g}}{\sigma_{w_g}} = \frac{\sigma_{u_g}}{\sigma_{w_g}} = \sqrt{\frac{L_u}{L_W}} = \sqrt{\frac{673}{100}} = 2.59 \tag{10}$$

The probability of occurrence of the gust intensities σ_{w_g} at various altitudes is represented by $P(\sigma_{w_g})$, defined as the exceedance probability

$$P(\sigma_{w_g}) = P_1 \hat{P}(\sigma_{w_g}) \tag{11}$$

where P_1 is the probability of occurrence of clear air turbulence, and

$\hat{P}(\sigma_{w_g})$ is the probability of equalling or exceeding a given magnitude of σ_{w_g} once clear air turbulence is encountered.

The probability of occurrence of clear air turbulence, P_1, at various altitudes is defined by the curve in Fig. 6 derived from various measurements. According to Fig. 6, $P_1 = 0.8$ at 100 ft.

The probability $\hat{P}(\sigma_{w_g})$ of equalling or exceeding a given σ_{w_g} is depicted by the curve in Fig. 7.

B. DETERMINISTIC GUSTS

1. Wind Shears

Although horizontal wind shear near the ground is a relatively common phenomenon, it is still not fully understood. This is due, in part, to the paucity of shear measurements. As a result, such things as probability of encounter, and distribution of shear magnitudes at various altitudes are not presently known. Another reason for the lack of a better understanding of wind shears is that shear can result from a number of different causes. Probably the best understood cause of horizontal wind shear is the boundary layer effect of the ground on a moving air mass. Thus, the air closest to the ground moves slower than the air higher up. This primary effect then leads to a secondary effect because of the so-called Coriolis forces. The net result is that the wind shifts in direction in addition to decreasing in magnitude. This is a familiar situation to student pilots who are taught that the wind direction will shift about 45 deg (counterclockwise) and the magnitude will drop by almost 50 percent during the final two thousand feet descent to a landing (Ref. 4). The explanation for this is that the wind tends to align itself with the pressure gradient (from high to low) near the ground, and to align itself with the Coriolis-produced "cyclonic" swirls (that are perpendicular to the pressure gradient) at higher altitudes. Figure 8 depicts this situation simply.

A sample of British data (Ref. 5) for shear measurements is presented next to indicate the measured probability distribution of shears over relatively flat terrain. Figure 9 shows a histogram of the average shear over a height range of 15 meters down to 1 meter. Superimposed on the histogram is a Gaussian probability curve having a mean and rms deviation from the
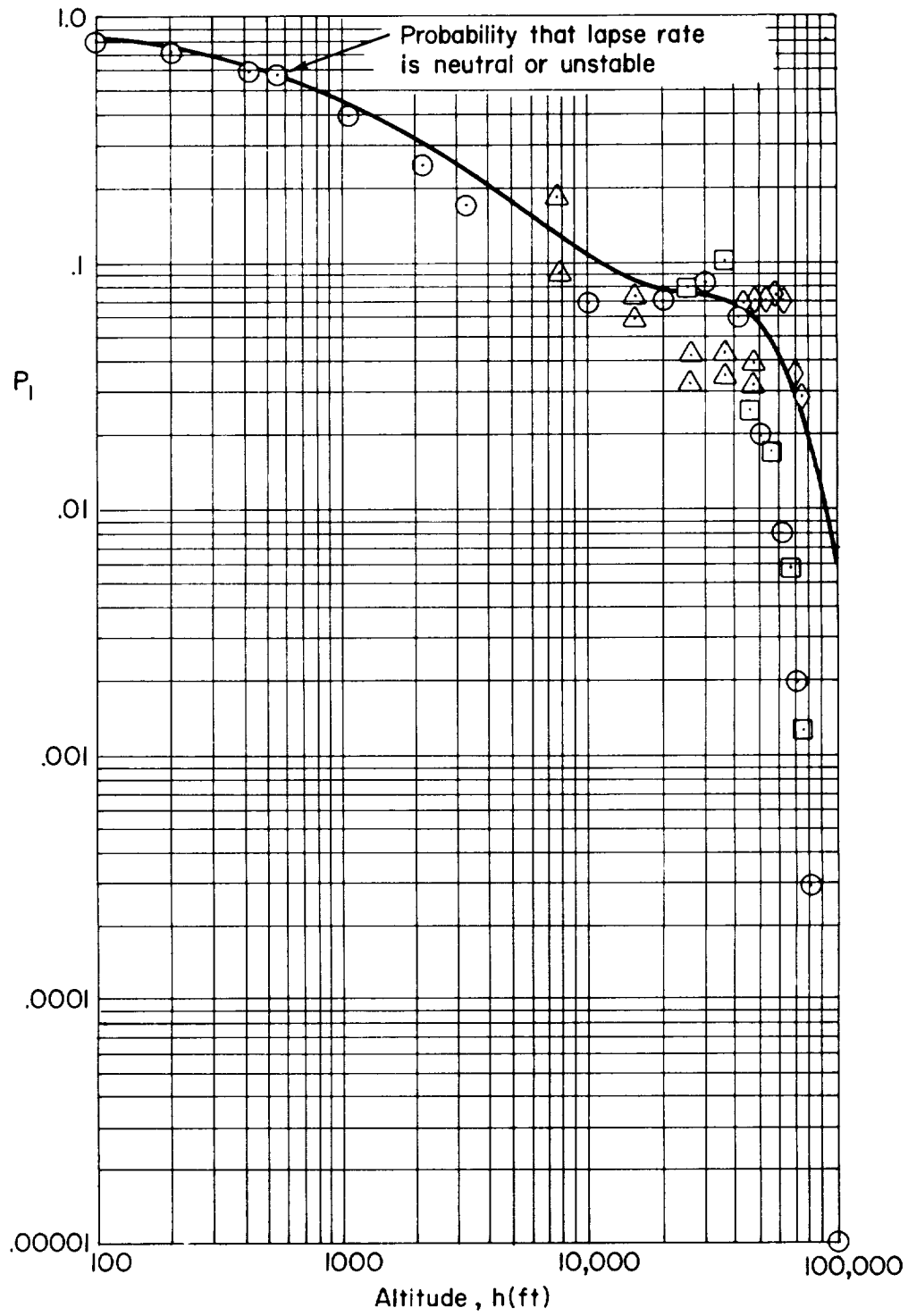
Figure 6. Probability P_1 of Encountering Turbulence

17
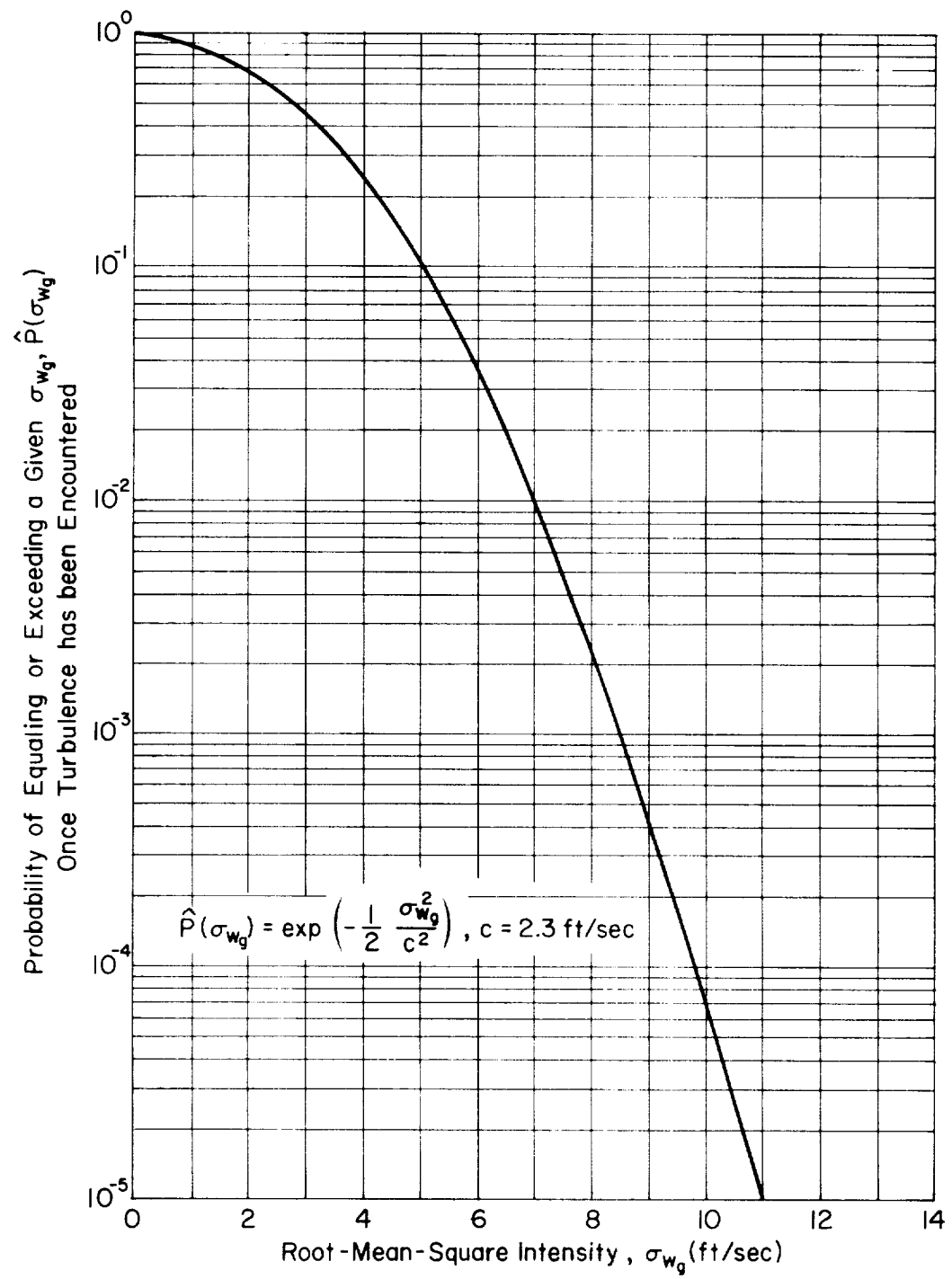
Figure 7. Exceedance Probability for σ_{W_g}

The plot is labeled with axes:
- Y-axis: Probability of Equaling or Exceeding a Given σ_{w_g}, $\hat{P}(\sigma_{w_g})$ Once Turbulence has been Encountered
- X-axis: Root-Mean-Square Intensity, σ_{w_g} (ft/sec)

Equation on plot:
$$\hat{P}(\sigma_{w_g}) = \exp\left(-\frac{1}{2}\frac{\sigma_{w_g}^2}{c^2}\right), \ c = 2.3 \ ft/sec$$
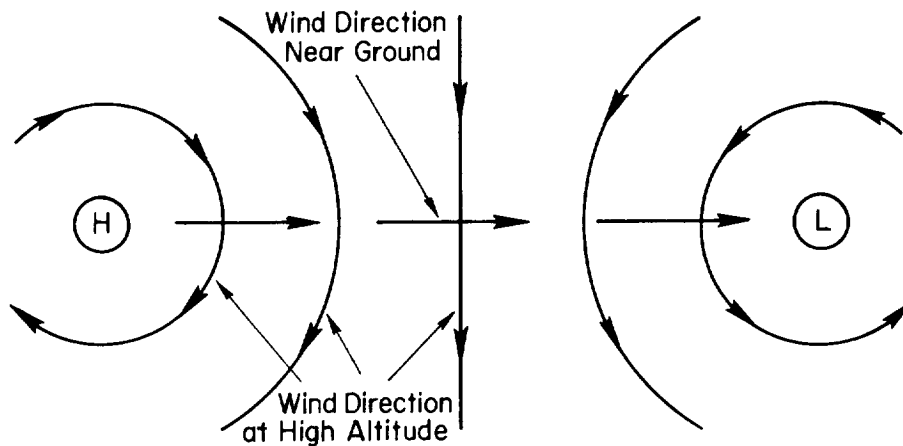
Figure 8 . Idealization of Wind Directions Near the Ground
and at High Altitude (in the Northern Hemisphere)

mean equal to that computed from the data comprising the histogram. A
similar figure for average shear over an altitude range of 75 meters down
to 30 meters is given in Fig. 10. Figures 11 and 12 then follow with
cumulative probability plots to test the data for being Gaussian. As
seen in these plots, the data appears to be reasonably Gaussian over the
ranges measured.

It is pertinent here to make a few comments regarding wind shear
measurements. Tower data (giving simultaneous wind speed measurements
at several altitudes) has consistently led to smaller shear values than
is computed from instrumentation aboard a descending airplane. Although
a purist may regard the tower data as the more appropriate method for
obtaining accurate shears, it is really the effect on the airplane that
is of interest. That is, the quantity actually desired is the rate of
change of wind along the airplane's flight path (and not the wind gradient
measured vertically over a single point on the ground at a given instant
in time). Thus, the technical problems of measuring "accurate" wind shears
is confounded by a semantic problem as well. Strictly speaking, a wind
shear is the instantaneous vertical gradient of horizontal wind. But, in
addition to this type of wind variation, an airplane may experience a
change in horizontal wind due to a longitudinal gradient, or even due to

19
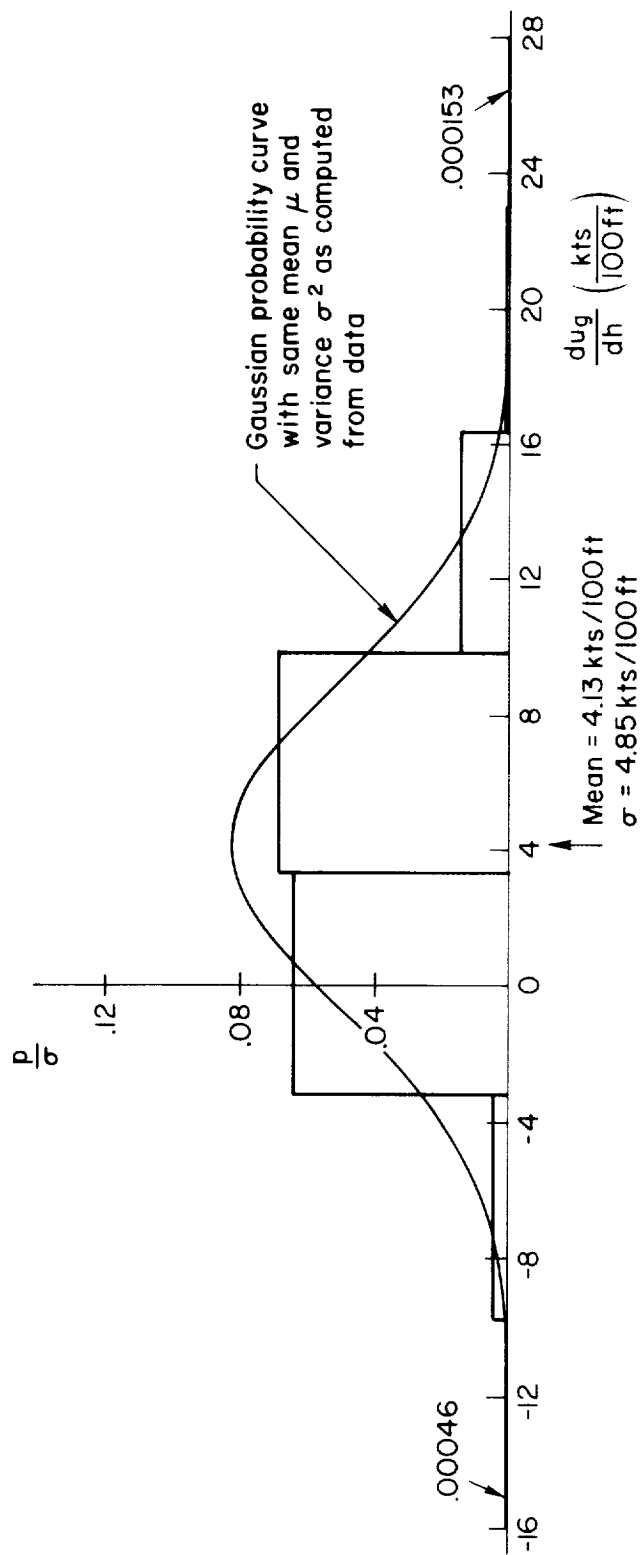
Figure 9. Probability Distribution of Measured Wind Shears from Ref. 3
($1 \leq h \leq 15$ meters)
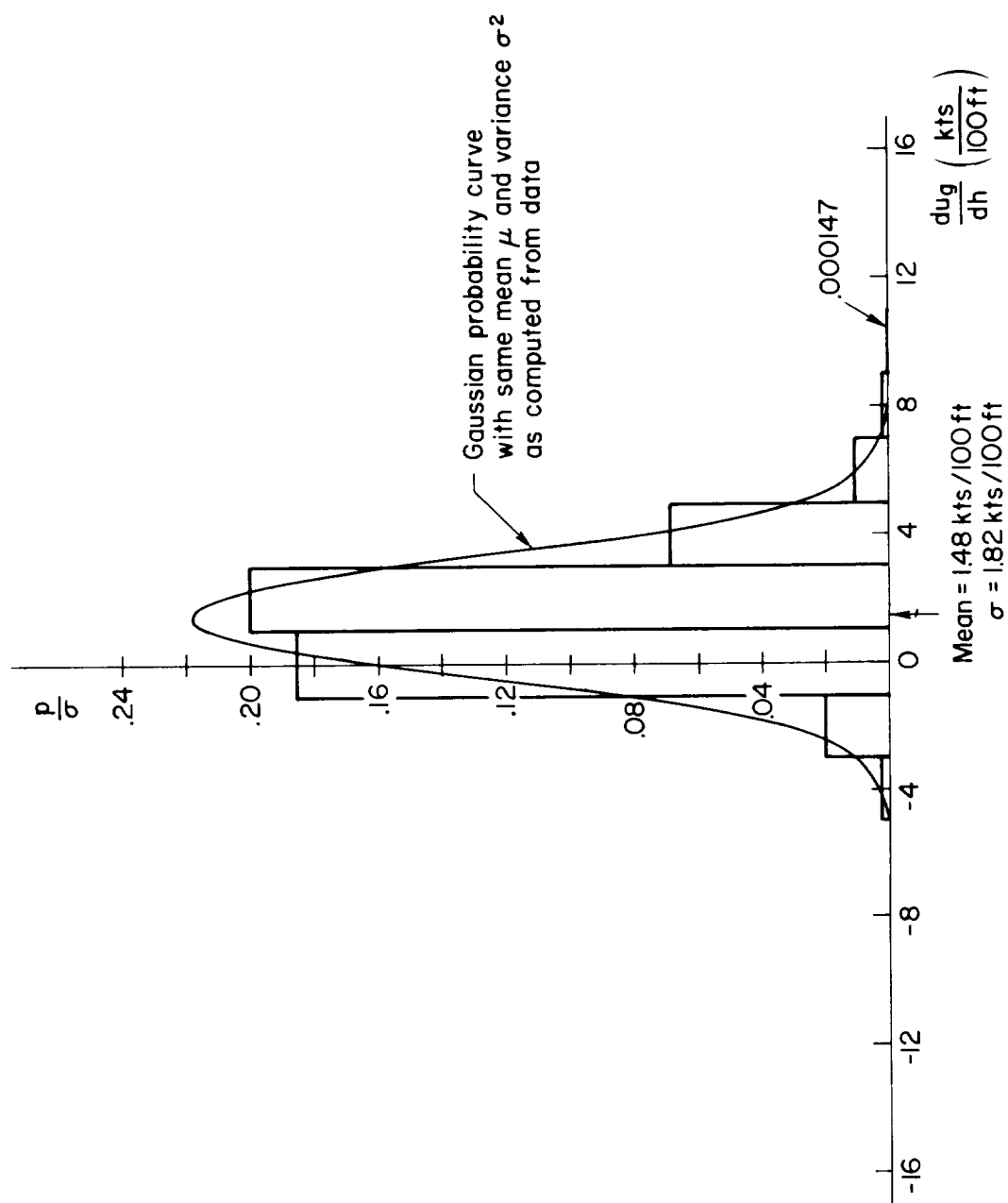
Figure 10. Probability Distribution of Measured Wind Shears from Ref. 5
($30 \leq h \leq 70$ meters)
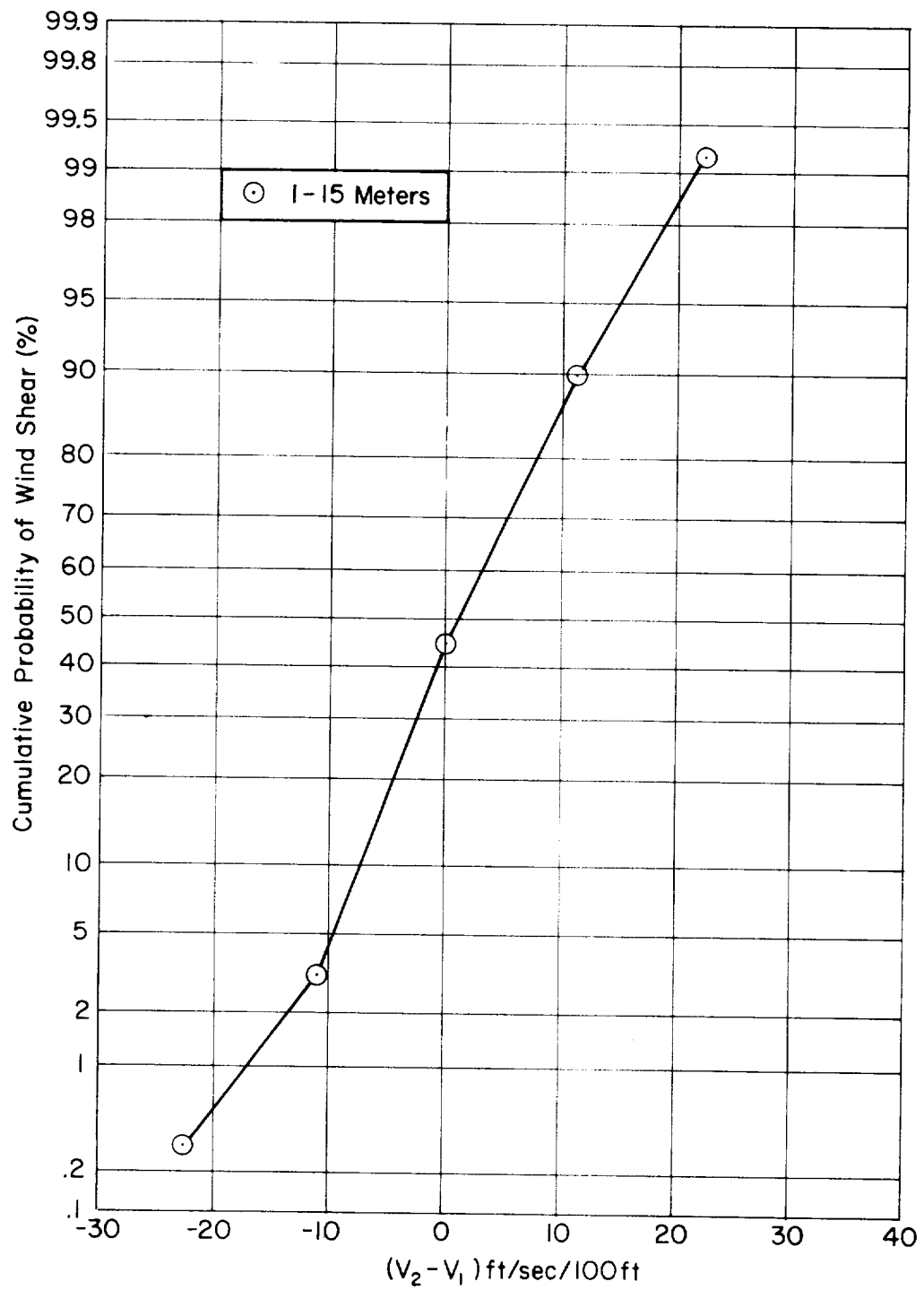
Figure 11.   Cumulative Probability of Measured Wind Shears
from Ref. 9 ($1 \le h \le 15$ meters)
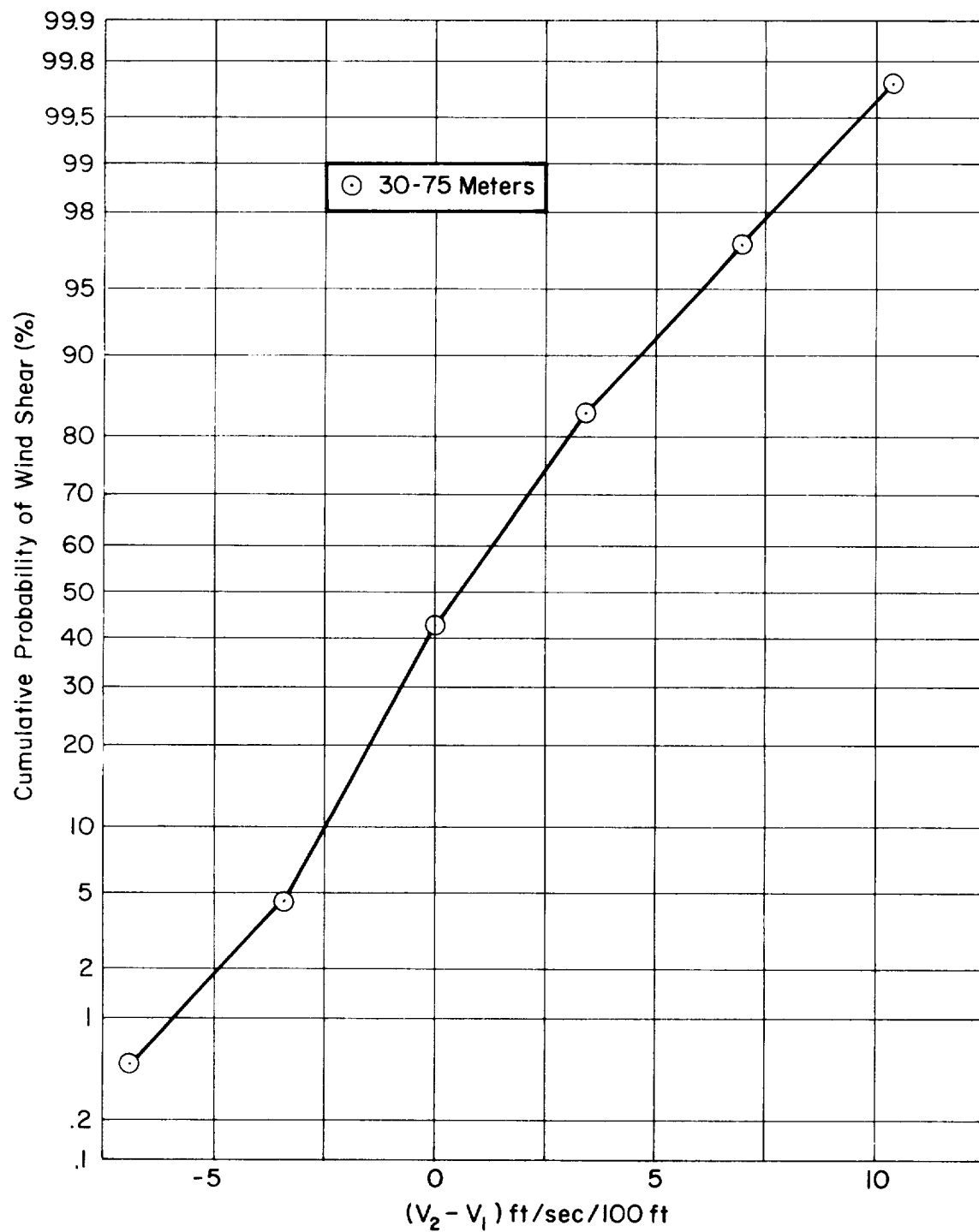
Figure 12. Cumulative Probability of Measured Wind Shears
from Ref. 5 (30 ≤ h ≤ 75 meters)

23

a wind fluctuation as a function of time (which may have no spatial gradient), or to any combination of these possibilities. When thought of in this light it seems reasonable that the effect of a true vertical gradient may actually be minor compared to the other effects. However, whether it is or not is really not of concern here. What is important is to recognize that tower data is not truly representative of the magnitude of horizontal wind changes that are commonly experienced by an airplane during final approach.

It may be useful at this time to present some direct quotations from Ref. 6 pertaining to Lear Siegler, Inc., experience with automatic landings in the Caravelle. In particular, the following concerns the occurrence of large wind shears near the ground.

> "The experience obtained during the LSi/SUD program indicates that this gradient in practice is much more severe than generally accepted, and it also appears that this gradient becomes more severe as the altitude decreases, due to the effects of the ground on the air mass. Fore and aft wind shears of 30 knots per 100 feet of altitude, lasting for periods of eight seconds, have actually been recorded by rather complete instrumentation on at least three of the automatic landings made in Toulouse. The terrain at Toulouse is relatively level, and would not be considered conducive to causing such wind shears. The weather conditions at the time these occurrences were recorded did not appear to be abnormal."

> "Experience on the LSi/SUD program has also indicated that wind gradients approaching the same magnitude appear in the lateral case. Crab angles of 15 degrees have been experienced at 150 to 200 feet of altitude with the touchdown occurring with a zero crab angle. At the approach speeds of the Caravelle, this is equivalent to a cross-wind gradient of 16 knots per 100 feet, which is far in excess of four knots per 100 feet."

> "The wind gradients actually experienced in the LSi/SUD program disagree with the information presented in RTCA SC-79, which is the source of the presently accepted four knots per 100 feet. However, the larger figures obtained on the LSi/SUD program are not the result of an isolated occurrence; also, they are well documented, and as such should be considered valid."

Taking into consideration all of the above information on shear, "standard" shear inputs were selected for the longitudinal and lateral situations. For our calculations, wind shear is simulated by introducing

an altitude dependent steady wind — for both the headwind and crosswind
components. For the headwind component the variation with altitude
starts at 200 ft and is linear down to an altitude of 100 ft. Changes
in the magnitude of the headwind shear occur at 100 ft and 50 ft, as
shown in Fig. 13. The crosswind component also starts at 200 ft and has a
linear variation with altitude down to the ground, as also shown in
Fig. 13. Although the magnitudes shown may be considered somewhat
arbitrary, they are representative of actual measured shears, and are
consistent with current thinking in the industry concerning autopilot
requirements for Category III conditions.

Having presented a model for random gusts, then a short discussion
on shear, followed by some measured shear data, and, finally, the comments
of an autopilot designer and test pilot, it is now of interest to present
a casual consensus of the aircraft industry's unofficial thinking on over-
all environmental condition limits for automatic approach and landing sys-
tems. Table III contains such a consensus. It is noted that "patches" of
turbulence and discrete gusts (such as steps and 1 − cosine pulses) are not
commonly included in the environmental conditions pertinent to approach and
landing.

TABLE III

CONSENSUS OF ENVIRONMENTAL CONDITION LIMITS
FOR AUTOMATIC APPROACH AND LANDING

PARAMETER	LIMITS
Steady Wind	25 kt headwind 10 kt tailwind 15 kt crosswind
Turbulence	Moderate: 6-1/2 ft/sec — 9 ft/sec rms w_g

Shear	u_g: −4 kts/100 ft $100 \text{ ft} \leq h \leq 200 \text{ ft}$
	         −8 kts/100 ft $50 \text{ ft} \leq h \leq 100 \text{ ft}$
	        −25 kts/100 ft $0 \leq h \leq 50 \text{ ft}$
	v_g: 15 kts/100 ft $0 \leq h \leq 100 \text{ ft}$
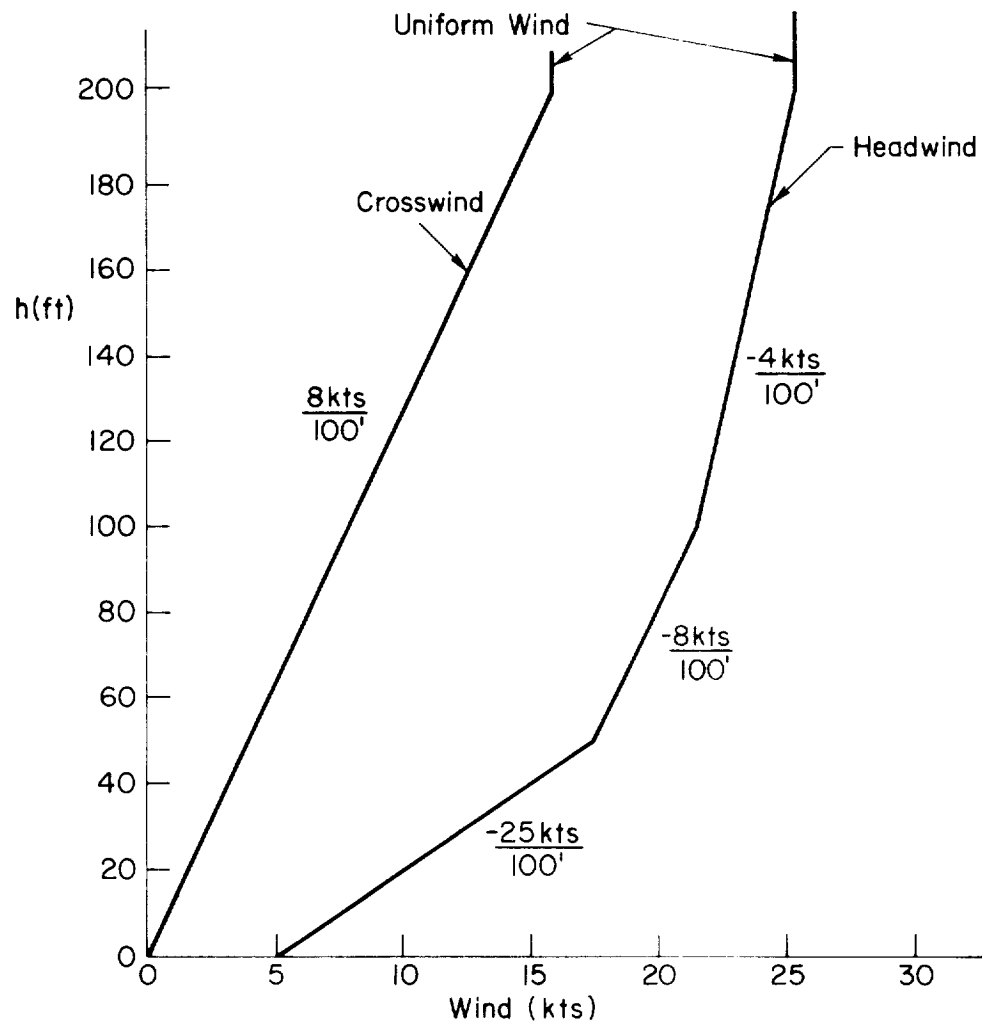
Figure 13. Wind Profiles (Showing Shear)

2. Step Gusts and 1-Cos Gusts

In addition to random gusts and shears, steps and 1-cosine gusts should also be considered. The 1-cosine gusts are included to represent the large discrete gust pulses that occasionally occur in turbulent air, but that are not appropriately included in the random gust or wind shear model inputs. The same magnitude was selected for all three gust components (u_g, v_g, w_g), namely, 15 kt at the peak. This corresponds to the U. S. Weather Bureau's definition of moderate turbulence (where peak gust magnitude is between 20 ft/sec and 35 ft/sec). The duration of the 1-cosine pulse is 2.5 sec, which corresponds roughly to the time to travel 25 chord lengths (Ref. 7).

Step gusts are included to represent the occasional very long lasting gusts. Because the longer lasting vertical gusts near the ground are not as large as the horizontal ones, and because the longer lasting horizontal gusts are caused primarily by changes in the "total" wind, the magnitudes selected for the step gusts are different for all three components. The u_g and v_g steps were chosen to be 12 kts and 7 kts, respectively — which corresponds closely to a 50 percent decrease in the total wind magnitude for the case of a steady wind having headwind and crosswind components as given in Table III. The 7 kt crosswind component also agrees with the crosswind gust environment specified for the C-141 in Ref. 8, although for the C-141 the requirement was for a steady 25 kt crosswind — gusting to 32 kts. The 5 kt w_g step was selected primarily on the basis of Ref. 9 which suggested it as a "realistic condition." Note that this makes the w_g component the smallest of the three, per the earlier comment regarding the relation between long lasting horizontal and vertical gusts. All of the selected inputs are summarized in Table IV at the end of this section.

C. ILS BEAM NOISE

The effects of beam noise, for both the localizer and glide slope signals, can be determined by exciting the system with beam noise inputs. A localizer noise input was obtained from average power spectral density plots of beam noise for localizers at several airports. Plots for conventional and directional localizer noise are

repeated here as Figs. 14 and 15 for easy reference. These spectral den-
sity plots were scaled so that their integrals give the mean-squared value,
i.e.,

$$\sigma^2 = \int_0^\infty \Phi(\omega)d\omega \qquad (12)$$

Using Eq. 12 and the plots in Figs. 14 and 15 leads to the result
that the noise for the "average" localizer is of the order of 5 μa rms.
This exceeds the Category II requirement of 2.5 μa rms, and therefore
cannot be used directly. However, for model purposes a localizer noise
power spectrum was obtained by fitting a simple analytical expression
to the shape of the directional localizer, and then scaling down the
rms level to 2.5 μa (as shown by the dashed line in Fig. 15).

We were unable to find an existing power spectral density plot for
glide slope beam noise. Therefore, we obtained some glide slope beam
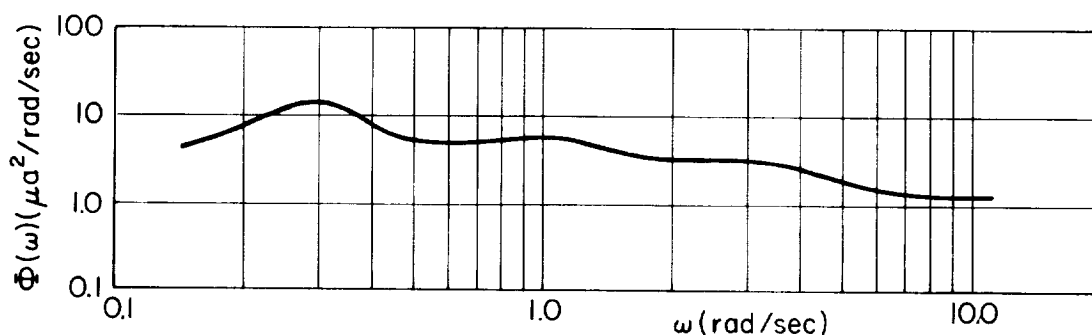
Figure 14. Average Conventional Localizer Power Spectral Density
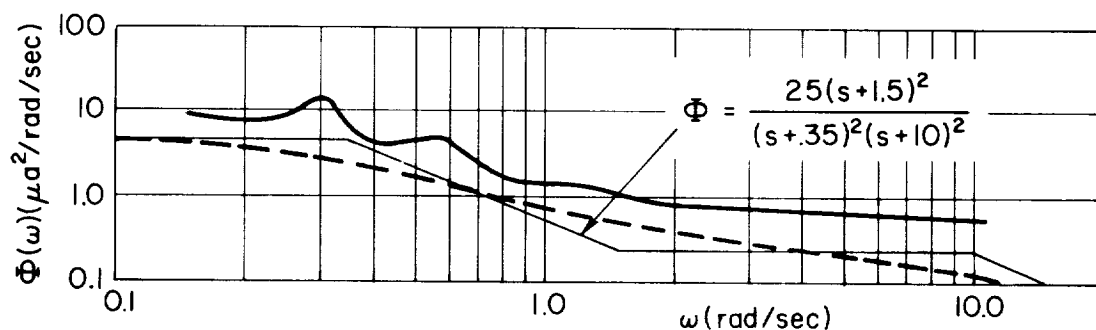
Figure 15. Average Directional Localizer Power Spectral Density

28

data from the FAA and analyzed it ourselves to obtain a PSD plot. The glide slope noise data came from measurements at LaGuardia made by the FAA in January of 1967. This particular beam just meets Category II criteria from the outer marker down to the middle marker, and therefore the PSD plot pertinent to this segment of the beam is the one used here. The PSD plot is given in Fig. 16 along with a data fit by a simple analytical expression.
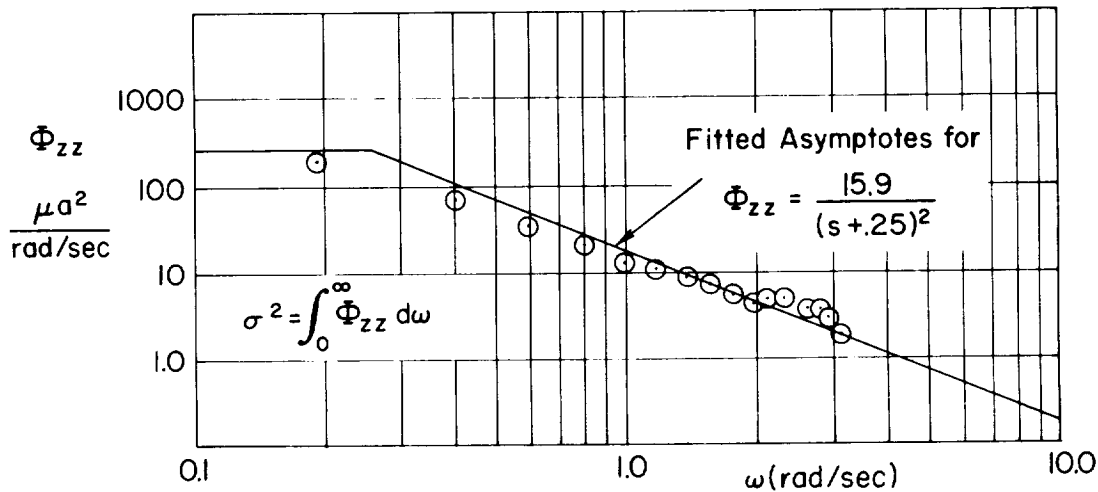
Figure 16. Power Spectral Density Plot of Glide Slope Beam Noise at LaGuardia (from Outer Marker to Middle Marker at Low Tide) — RMS Level is 10 μa

It is noted that a short-time-stationarity argument similar to that used earlier for random gusts can be applied to beam noise. That is, even though the noise properties may be range-dependent, they are relatively stationary over intervals of the order of airplane/system settling times, and can therefore be treated as stationary inputs.

It is pertinent here to point out that criteria for maximum allowable beam noise are currently specified only in terms of mean beam angle, maximum bend amplitude, and rms deviation from the mean. However, for simulation purposes it is necessary to know also the amplitude and frequency distributions of the noise. (For example, a beam may have a Gaussian amplitude probability distribution and a band-limited white-noise frequency distribution.)

TABLE IV

SUMMARY OF STANDARD INPUTS

	ALTITUDE RANGE ENCOUNTERED	MAGNITUDES OF PARAMETERS	
		LONGITUDINAL	LATERAL
RANDOM GUSTS	Down to 100'	$\sigma_{u_g} = 2.59\ \sigma_{w_g}$ σ_{w_g} is given in Fig. 7	$\sigma_{v_g} = \sigma_{u_g}$
WIND SHEARS	200' to 100'	$\dfrac{du_g}{dh} = \dfrac{-4\ \text{kts}}{100'}$	$\dfrac{dv_g}{dh} = \dfrac{8\ \text{kts}}{100'}$
	100' to 50'	$\dfrac{du_g}{dh} = \dfrac{-8\ \text{kts}}{100'}$	$\dfrac{dv_g}{dh} = \dfrac{8\ \text{kts}}{100'}$
	50' to ground	$\dfrac{du_g}{dh} = \dfrac{-25\ \text{kts}}{100'}$	$\dfrac{dv_g}{dh} = \dfrac{8\ \text{kts}}{100'}$
STEP GUSTS	150' to ground 50' to ground	$\Delta u_g = 12\ \text{kts}$ $\Delta w_g = 5\ \text{kts}$	$\Delta v_g = 7\ \text{kts}$
1-COS GUSTS	150' 50'	Peak $u_g = 15$ kts, $T = 2.5$ sec Peak $w_g = 15$ kts, $T = 2.5$ sec	Peak $v_g = 15$ kts, $T = 2.5$ sec
BEAM NOISE	1,500' to 50' 1,500' to ground	$\sigma_{g/s} = 10\ \mu a$	$\sigma_{LOC} = 2.5\ \mu a$

SECTION IV

DERIVATION OF APPROACH OUTCOME PROBABILITIES

One of the key aspects in the presentation of a terminal area model is a definition of the model outputs. This was accomplished in Table I (repeated here for ease of reference) which lists the "basic outcomes" for an approach, and their associated measures, metrics, and critical limits. The metrics are computed from the dynamic portion of the aircraft/approach-system model. Then, by comparing the metrics with the appropriate critical limits, figures of merit in the form of outcome probabilities are computed. The various outcome probabilities are a basis for comparing competing systems, as well as a means for evaluating the effects of inputs and/or changes in system components.

Figure 17 shows an approach outcome tree which indicates how aircraft dispersions can lead to the various approach outcomes listed in Table I. Although this figure is somewhat oversimplified, it does indicate conceptually how a model can be constructed to give approach outcomes as outputs. Before proceeding to a more detailed breakdown of the model, a digression to clarify the definitions of the accidents listed in Table I is pertinent.

A. DETAILED DISCUSSION OF TYPES OF APPROACH OUTCOMES

During an approach more than one of the basic outcomes listed in Table I may occur. For example, a hard landing and running off the runway could both occur on the same landing. However, for such a situation one might still consider this to be a single accident because it is not surprising to find that an airplane ran off the runway after a particularly hard landing (where the landing gear failed). Thus the "critical" outcome can be considered to be a hard landing (for this case) even though another of the basic outcomes also actually occurred. Another example of a combination of basic outcomes would be landing short and having an excessive crab angle (enough to break the landing gear). Clearly, the fact that an excessive crab angle was present would go unnoticed if an airplane touched down on somebody's garage roof a mile short of the threshold. Thus the critical outcome for a combination of these two basic outcomes is the short

31

TABLE I

CONSIDERATIONS FOR APPROACH AND LANDING OUTCOMES

BASIC OUTCOME	ASSOCIATED PERFORMANCE MEASURES	PERFORMANCE METRICS	CRITICAL LIMITS (To achieve outcome)	OUTCOME PROBABILITIES (These are functions of performance metrics and critical limits)	COMMENTS
Successful landing	Dispersions at decision height and/or reference position and at touchdown	μ_h, σ_h, μ_y, σ_y, μ_u, σ_u, μ_E, σ_E	Airplane must be within successful-landing "window"	P_{OK}	Because successful landings and missed approaches will account for almost all approaches, P_{MA} will be a very significant parameter. $$(P_{OK} \doteq 1 - P_{MA})$$
Successful missed approach	Dispersions at decision height	μ_h, σ_h, μ_y, σ_y, μ_u, σ_u, μ_E, σ_E	Airplane must be outside of successful approach window but within successful "go-around" window	P_{MA}	
Short landing	Longitudinal touchdown location	$\mu_{x_{TD}}$, $\sigma_{x_{TD}}$	$x_{TD} < x_{TD_{MIN}}$	P_{SL}	The sum of the various accident probabilities will be considerably smaller than P_{MA}. (The sum should be of the order of 10^{-6} or smaller.)
Hard landing	Sink rate at touchdown	$\mu_{\dot{h}_{TD}}$, $\sigma_{\dot{h}_{TD}}$	$|\dot{h}_{TD}| > |\dot{h}_{TD}|_{MAX}$	P_{HL}	
Overrun runway during rollout	Airspeed and altitude errors at reference position	μ_E, σ_E	$\left. \begin{array}{c} K_1\Delta h_R + K_2\Delta u_R > E_{MAX} \\ E \end{array} \right\}$	P_{OR}	
Land off side of runway	Lateral touchdown location	$\mu_{y_{TD}}$, $\sigma_{y_{TD}}$	$|y_{TD}| > y_{TD_{MAX}}$	P_{LO}	
Drag a wing tip or engine pod during landing	Bank angle at touchdown	$\mu_{\varphi_{TD}}$, $\sigma_{\varphi_{TD}}$	$\varphi_{TD} > \varphi_{TD_{MAX}}$	P_{DW}	
Land with excessive misalignment angle (putting side loads on landing gear)	Side velocity at touchdown	$\mu_{v_{TD}}$, $\sigma_{v_{TD}}$	$|v_{TD}| > v_{TD_{MAX}}$	P_v	
Run off side of runway during rollout	Lateral displacement deviations during rollout	$\mu_{y_{RO}}$, $\sigma_{y_{RO}}$	$|y_{RO}| > y_{RO_{MAX}}$	P_{RO}	

Figure 17. Simplified Version of Approach Outcome "Tree" (General Breakdown of Possible Approach Consequences)

TABLE V

DEFINITIONS OF "CRITICAL" APPROACH OUTCOMES[*]

BASIC OUTCOMES (AND ABBREVIATIONS)		CRITICAL OUTCOMES RESULTING FROM ANY TWO BASIC OUTCOMES[†]								
Successful Landing	OK	OK								
Successful Missed Approach	MA	—	MA							
Short Landing	SL	—	—	SL						
Hard Landing	HL	—	—	SL	HL					
Overrun Runway During Rollout	OR	—	—	SL	HL	OR				
Land Off Side of Runway	LO	—	—	SL	LO	LO	LO			
Drag a Wing Tip or Engine Pod During Landing	DW	—	—	SL	HL	DW + OR	LO	DW		
Land with Excessive Misalignment Angle	v	—	—	SL	HL	v	LO	DW + v	v	
Run Off Side of Runway During Rollout	RO	—	—	SL	HL	RO	LO	DW + RO	v	RO
		OK	MA	SL	HL	OR	LO	DW	v	RO
		BASIC OUTCOMES								

[*]For situations where an approach results in more than one of the basic outcomes.

[†]A basic outcome from the left column paired with a basic outcome at the bottom gives the critical outcome shown in the box for that row and column.

landing. On the other hand, some combinations of basic outcomes deserve joint consideration if they occur on the same approach. Table V presents the critical outcomes for all possible pairs of basic outcomes. A list of the different critical approach outcomes from Table V is then given in Table VI.*

At this point it is convenient to neglect the combination of dragging a wing tip and overrunning the runway. This is not unreasonable because overrunning a runway is usually so much more serious than dragging a wing tip that if the two occurred on the same landing the dragged wing tip could easily be lost in the confusion. The convenience arises because the outcomes can now be separated into longitudinal and lateral situations, as shown in Table VII.

TABLE VI

LIST OF POSSIBLE CRITICAL
APPROACH OUTCOMES

OK
MA
SL
HL
OR
OR + DW
LO
DW
v
RO
DW + v
DW + RO

Before getting back to the detailed breakdown of the model, it is pertinent to present some of the results of our investigation of accident and incident statistics for several recent years. (A detailed presentation of accident and incident statistics is given in Appendix A.) One of the purposes of the investigation was to determine the relative likelihood of the various outcomes considered in Table I. In this way we could learn which outcomes were most important and which ones were of least importance. Table VIII shows those outcomes from Table I for which data is available, and their relative likelihoods (based on the landing accidents and incident for 1964 through 1966 for U. S. air carriers).

---

*Our selection of critical outcomes is done to make our outcome definitions consistent with those used in publishing accident and incident data.

TABLE VII

SUMMARY OF CRITICAL APPROACH OUTCOMES

Longitudinal Situation	Lateral Situation
OK: Successful Landing	OK: Successful Landing
MA: Successful Missed Approach	MA: Successful Missed Approach
SL: Short Landing	LO: Land Off Side of Runway
HL: Hard Landing	DW: Drag a Wing-Tip (or Engine Pod) During Landing
OR: Overrun Runway During Rollout	v : Land with Excessive Misalignment Angle
	RO: Run Off Side of Runway During Rollout
	DW + v) Drag a Wing-Tip and Land with Excessive Misalignment
	DW + RO) Drag a Wing-Tip and Run Off Side of Runway

TABLE VIII

RELATIVE FREQUENCY OF BASIC OUTCOMES
FOR U. S. AIR CARRIERS DURING 1964 — 1966

	NUMBER OF ACCIDENTS/INCIDENTS	PERCENT OF	
		ACCIDENTS	INCIDENTS
Short landing	19/18	33	12-1/2
Hard landing	12/18	21	12-1/2
Overrun runway (hydroplaning not a factor)	11/20	19	14
Drag a wing tip	1/17	2	12
Run off side of runway	2/58	4	40
Others	12/13	21	9

From Table VIII it is evident that dragging a wing tip and running off the side of the runway are two relatively common incidents, but are only rarely serious enough to be classed as accidents. This leaves short landings, hard landings, and runway overruns as the more serious outcomes (in severity and frequency). It is noted that these more serious outcomes are basically longitudinal situations. Whether this tendency will continue for Category II approaches is not known.

Having digressed to define the critical approach outcomes, to separate them into longitudinal and lateral situations, and to look quickly at their relative occurrences, we can now proceed with a more detailed breakdown of the model that was shown in Fig. 17. Figures 18 and 19 show the longitudinal and lateral approach outcome "trees," including all of the various types of accidents.

Conceptually, it is a simple step to generate "performance" trees from Figs. 18 and 19 by considering the probabilities associated with each of the blocks shown. The resulting performance trees are shown in Figs. 20 and 21. It is pointed out that in Figs. 18 through 21 several implicit assumptions have been made. These are:

- A missed approach is never elected when the airplane is within the landing window.
- A missed approach is always elected when the airplane is outside the landing window.
- Missed approaches are elected only when at the decision height, and they are always successful.

Although these assumptions are not strictly valid in real life (due to the human judgment factor), they can nevertheless still be made because they don't introduce undue bias in the computed results and because they involve pilot decision alone and not inherent aircraft/landing-system characteristics. Inclusion of such a decision element could be a future refinement to the basic model.

The next step in the analysis procedure is to compute the various probabilities that go into the boxes in Figs. 20 and 21.
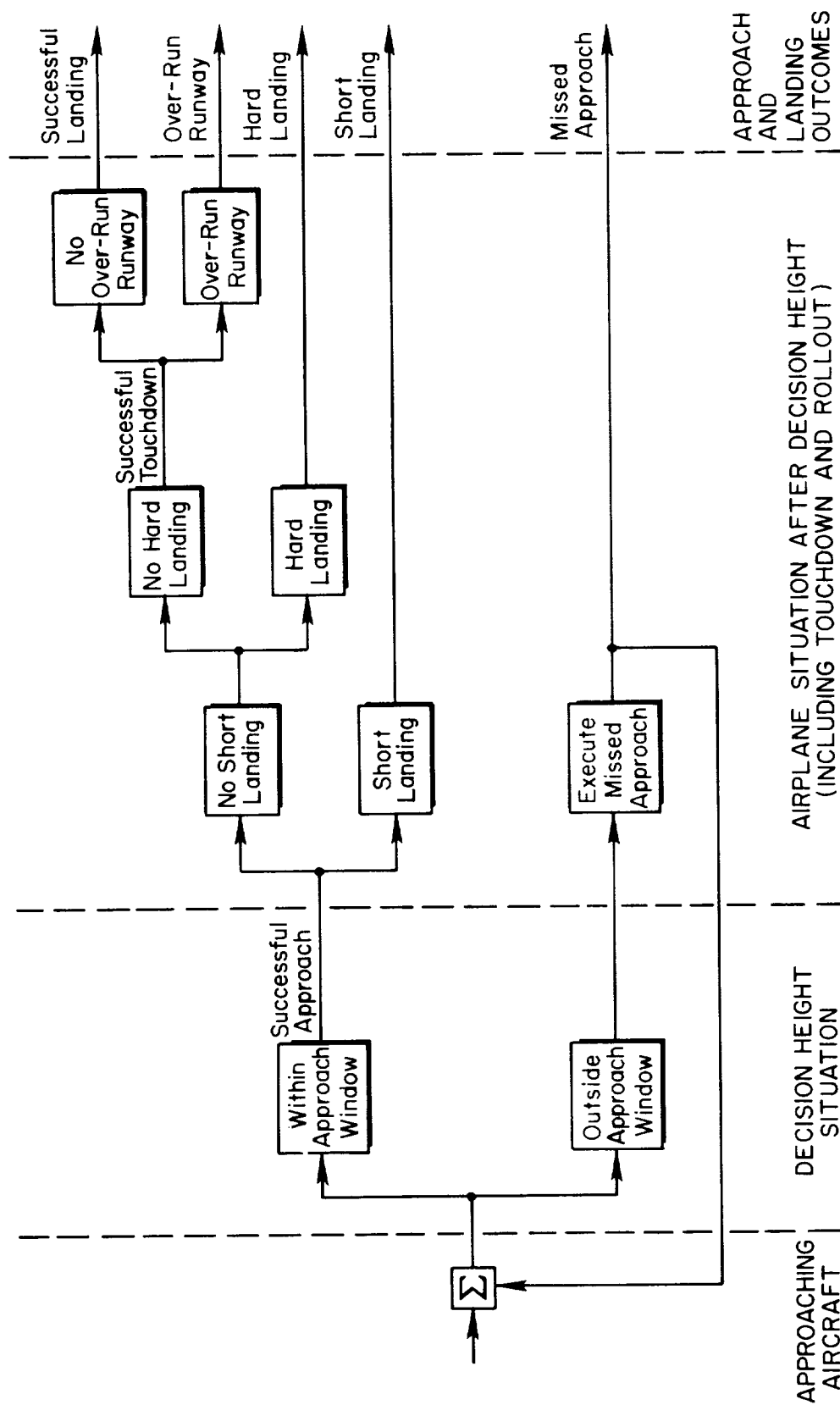
Figure 18. Longitudinal Approach Outcome "Tree"
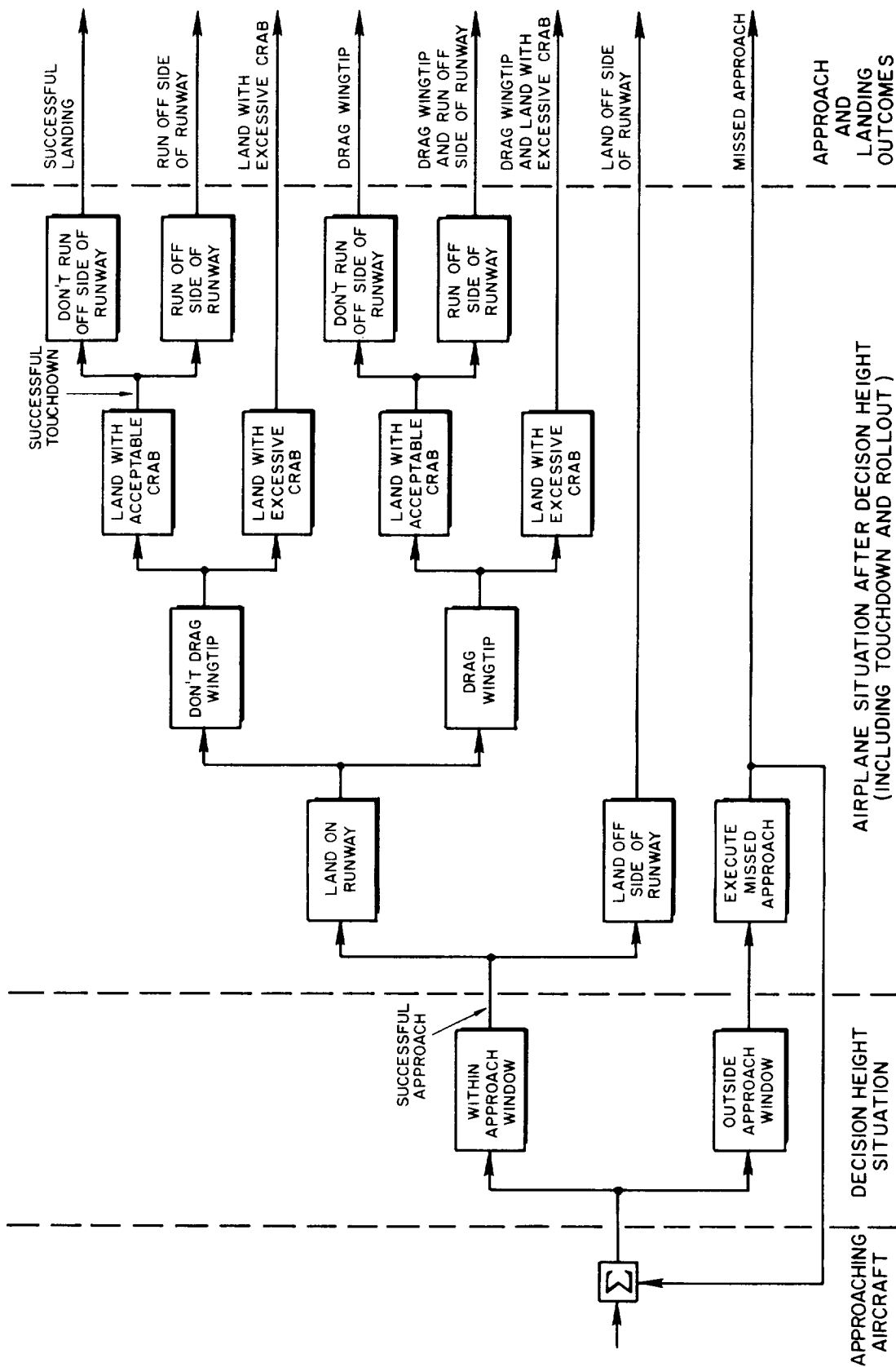
Figure 19. Lateral Approach Outcome "Tree"

39

Approaching Aircraft

Σ

$1-P_1$ — Successful Approach

P_1 — Outside Approach Window

$1-P_2$

P_2 — Short Landing

1 — Execute Missed Approach

$1-P_3$ — Successful Touchdown

P_3 — Hard Landing

Over-Run Runway

$1-P_4$ → Successful Landing (OK)

P_4 → Over-Run Runway (OR)

→ Hard Landing (HL)

→ Short Landing (SL)

→ Missed Approach (MA)
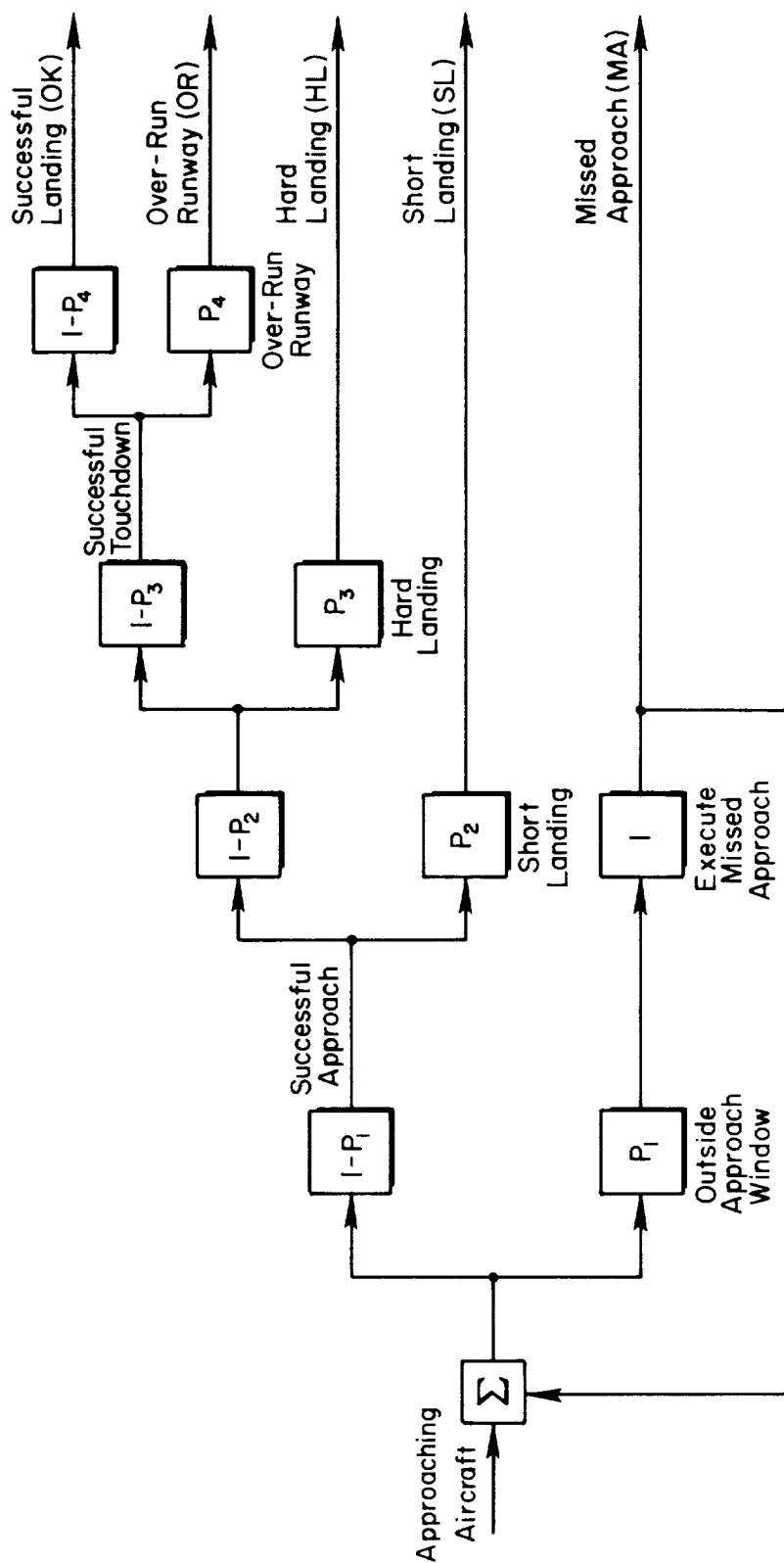
<u>LONGITUDINAL APPROACH AND LANDING OUTCOME PROBABILITIES</u>

$$P_{OK} = (1-P_1)(1-P_2)(1-P_3)(1-P_4)$$
$$P_{OR} = P_4(1-P_1)(1-P_2)(1-P_3)$$
$$P_{HL} = P_3(1-P_1)(1-P_2)$$
$$P_{SL} = P_2(1-P_1)$$
$$P_{MA} = P_1$$

<u>DEFINITIONS</u>

P_1 = Probability of being outside longitudinal approach window

P_2 = Probability of a short landing

P_3 = Probability of a hard landing, given that you did not have a short landing

P_4 = Probability of over-running runway, given that you made a successful touchdown

Figure 20. Longitudinal Approach and Landing Performance "Tree"

40

SUCCESSFUL LANDING (OK)

RUN OFF SIDE OF RUNWAY (RO)

LAND WITH EXCESSIVE CRAB (v)

DRAG WINGTIP (DW)

DRAG WINGTIP AND RUN OFF SIDE OF RUNWAY (DW + RO)

DRAG WINGTIP AND LAND WITH EXCESSIVE CRAB (DW + v)

LAND OFF SIDE OF RUNWAY (LO)

MISSED APPROACH (MA)

$1-P_5$

P_5 — RUN OFF SIDE

$1-P_5$

P_5 — RUN OFF SIDE

$1-P_4$

P_4 — EXCESSIVE CRAB

$1-P_4$

P_4 — EXCESSIVE CRAB

SUCCESSFUL TOUCHDOWN

$1-P_3$

P_3 — DRAG WINGTIP

$1-P_2$

P_2 — LAND OFF SIDE

SUCCESSFUL APPROACH

$1-P_1$ — OUTSIDE APPROACH WINDOW

P_1 — OUTSIDE APPROACH WINDOW

1 — EXECUTE MISSED APPROACH

Σ

LATERAL APPROACH AND LANDING OUTCOME PROBABILITIES

$P_{OK} = (1-P_1)(1-P_2)(1-P_3)(1-P_4)(1-P_5)$

$P_{RO} = P_5(1-P_1)(1-P_2)(1-P_3)(1-P_4)$

$P_v = P_4(1-P_1)(1-P_2)(1-P_3)$

$P_{DW} = P_3(1-P_1)(1-P_2)(1-P_4)(1-P_5)$

$P_{DW+RO} = P_3 P_5(1-P_1)(1-P_2)(1-P_4)$

$P_{DW+v} = P_3 P_4(1-P_1)(1-P_2)$

$P_{LO} = P_2(1-P_1)$

$P_{MA} = P_1$

DEFINITIONS

$P_1 \equiv$ PROBABILITY OF BEING OUTSIDE LATERAL APPROACH WINDOW

$P_2 \equiv$ PROBABILITY OF LANDING OFF SIDE OF RUNWAY

$P_3 \equiv$ PROBABILITY OF DRAGGING A WINGTIP, GIVEN THAT YOU LAND ON RUNWAY

$P_4 \equiv$ PROBABILITY OF HAVING EXCESSIVE SIDE VELOCITY, GIVEN THAT YOU LAND ON RUNWAY

$P_5 \equiv$ PROBABILITY OF RUNNING OFF SIDE OF RUNWAY, GIVEN THAT YOU LAND ON RUNWAY WITH ACCEPTABLE SIDE VELOCITY

Figure 21. Lateral Approach and Landing Performance "Tree"

B. EQUATIONS DEFINING APPROACH OUTCOME PROBABILITIES

The longitudinal and lateral situations will first be considered separately. Then these separate results will be used to obtain the combined probabilities (as required for the cases of missed approaches and successful landings).

Each of the probabilities of interest can be represented by an area under a probability density distribution curve. For Gaussian distributions these areas are simple to determine. They depend on only three parameters:

- The mean value of the pertinent variable
- The rms deviation from the mean
- The critical limits that define the accident (or whatever)

The example in Fig. 22 shows graphically how these quantities affect the probability of a short landing.

Figure 23 then defines the mathematical expression relating the shaded area to a numerical probability (for Gaussian distributions). The function F( ) can be looked up in a table or it can be computed via an algebraic expression.

Applying the relations in Fig. 23 to the example shown in Fig. 22 (assuming it to be Gaussian) gives the probability of a short landing as,

$$P_{SL} = 1 - F\left(\frac{-\mu x_{TD}}{\sigma_{x_{TD}}}\right) \tag{13}$$

or (because the Gaussian curve is symmetric)

$$P_{SL} = F\left(\frac{\mu x_{TD}}{\sigma_{x_{TD}}}\right) \tag{14}$$

Using the above technique gives the probability of a hard landing as,

$$P_{HL} = F\left(\frac{\mu \dot{h}_{TD} - \dot{h}_{TD_{max \ allowable}}}{\sigma_{\dot{h}_{TD}}}\right) \tag{15}$$
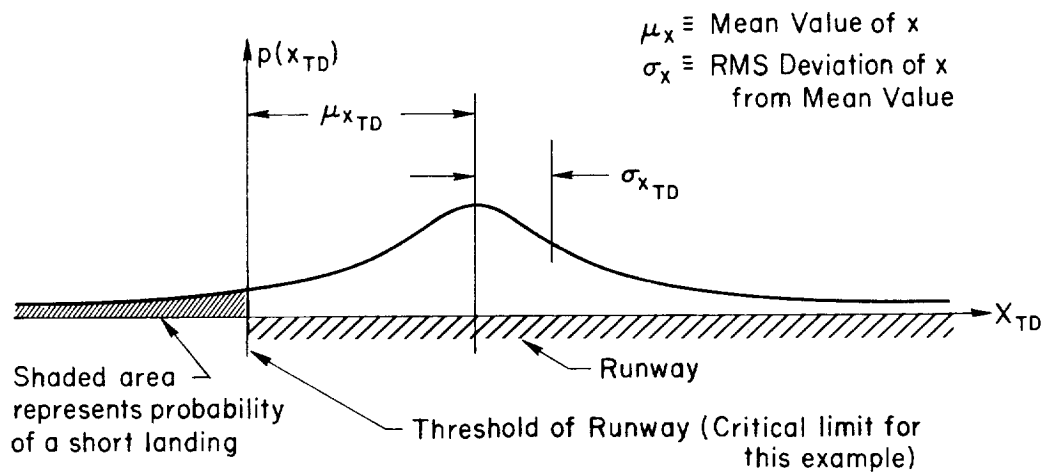
Figure 22. Graphical Presentation of Parameters Pertinent to the Computation of the Probability of a Short Landing
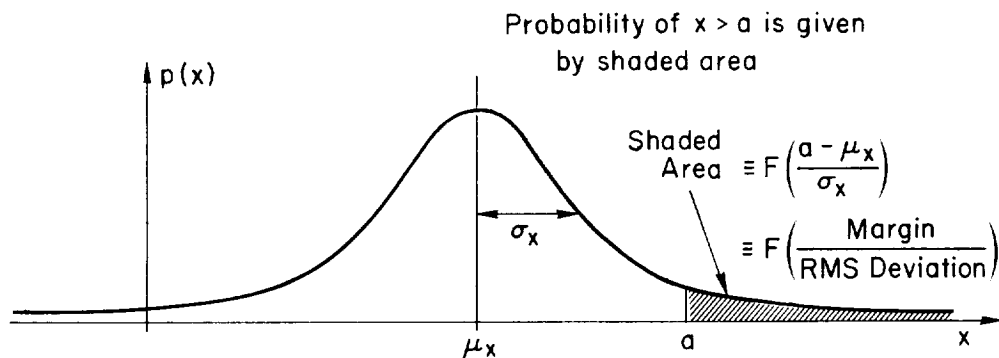
Figure 23. Definition of F( ) for a Gaussian Distribution

In a similar manner the probabilities of other touchdown accidents can also be expressed (assuming Gaussian distributions). However, rather than pursuing this further, we will take a slightly different approach at this point.

Accidents are very unlikely events and therefore accident probabilities are extremely small quantities. As a result, from a practical standpoint it is much more meaningful to consider the probability of a missed approach as a primary measure of a system's adequacy. This is supported by existing information indicating that at the Category II-B level the missed approach

43

rate can be as high as 40 percent. Thus, for practical purposes, making the Category II-B window a very large proportion of the time, say 95-99 percent, may be the most difficult part of the approach and landing sequence. Once this window is made, only the flare and removal of crab or wing-down are required to get on the ground with reasonable touchdown conditions. Therefore, the chance of an accident due to a short landing or an off-runway landing should decrease considerably in going from a Category I to a Category II window. However, most of the other outcome probabilities would be expected to be fairly similar to current operational experience. In any event, the considerations in the remainder of this report will be concerned only with determining the missed approach rate for various situations. In the next subsection the multidimensional approach window will be discussed.

C. DEFINITION OF APPROACH WINDOW

The purpose of an approach window is to define the critical limits for continuing an approach beyond the decision height. Once these limits are determined it is a relatively simple matter to express the probability of a missed approach in a concise form.

The approach window is defined in terms of three parameters: altitude, lateral displacement, and airspeed. Figure 24 shows the actual Category II window in space that the airplane must fly through at the 100 ft decision height (in addition to maintaining airspeed within the airspeed "window").

The values of the variables that were selected to define the longitudinal and lateral approach windows are:

$$d_{\epsilon_{max}} = 12 \text{ ft} \quad ; \quad y_{\epsilon_{max}} = 72 \text{ ft} \quad ; \quad \Delta u_{max} = 5 \text{ kts}$$

The d_ϵ and y_ϵ limits correspond to 75 microamps ($= 1$ dot) of glide slope error and 25 μa ($= 1/3$ dot) of localizer error at 100 ft altitude. (Full scale is ± 150 μa.) These are limits the FAA requires for Category II operation in Ref. 11. The airspeed limit was also selected on the basis of FAA criteria (Ref. 11). Note that the y_ϵ limits correspond to the centerline of the airplane being <u>within</u> the lateral confines of a typical 150 ft wide runway. This means that even if the airplane is at the edge
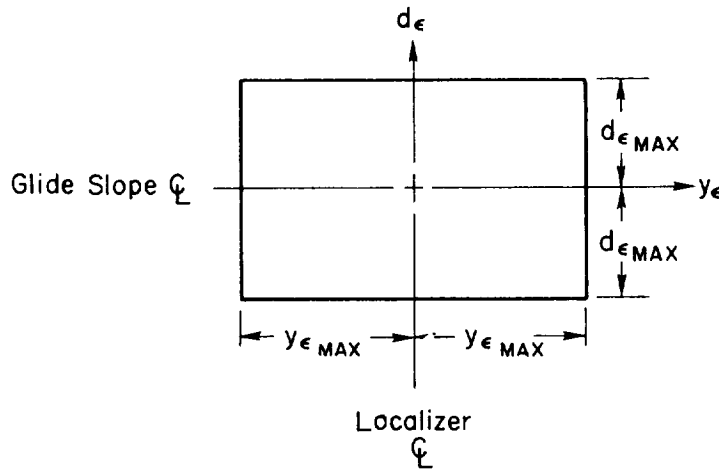
Figure 24. Category II Approach Window (at 100 ft Altitude)
for Vertical and Lateral Displacement Deviations

of the lateral window, only a small lateral correction is required to get both sets of main landing gear over the runway. At this point we might also note that a steady 12 ft altitude error on a 2.8 deg glide path corresponds to a longitudinal touchdown error of 246 ft, which still puts the airplane well within the acceptable landing zone.

D. EQUATIONS DEFINING THE PROBABILITY OF A SUCCESSFUL APPROACH

By making the assumptions of stationarity and normality (Gaussian) for the distributions of the random inputs (discussed in Section III), we can compute the means and rms deviations of the variables from their mean values (via the inputs and equations of motion). Then the probability density distribution plots, such as those shown in Fig. 25, can be used to determine the overall approach success probability as follows.

The probability of being outside the lateral limits of the approach window is given by the area under the tails of the lateral displacement distribution that falls outside the window limits. Thus,

$$P_{out-lat} = F\left(\frac{72 \text{ ft} + \mu_{y_\epsilon}}{\sigma_{y_\epsilon}}\right) + F\left(\frac{72 \text{ ft} - \mu_{y_\epsilon}}{\sigma_{y_\epsilon}}\right) \tag{16}$$

45
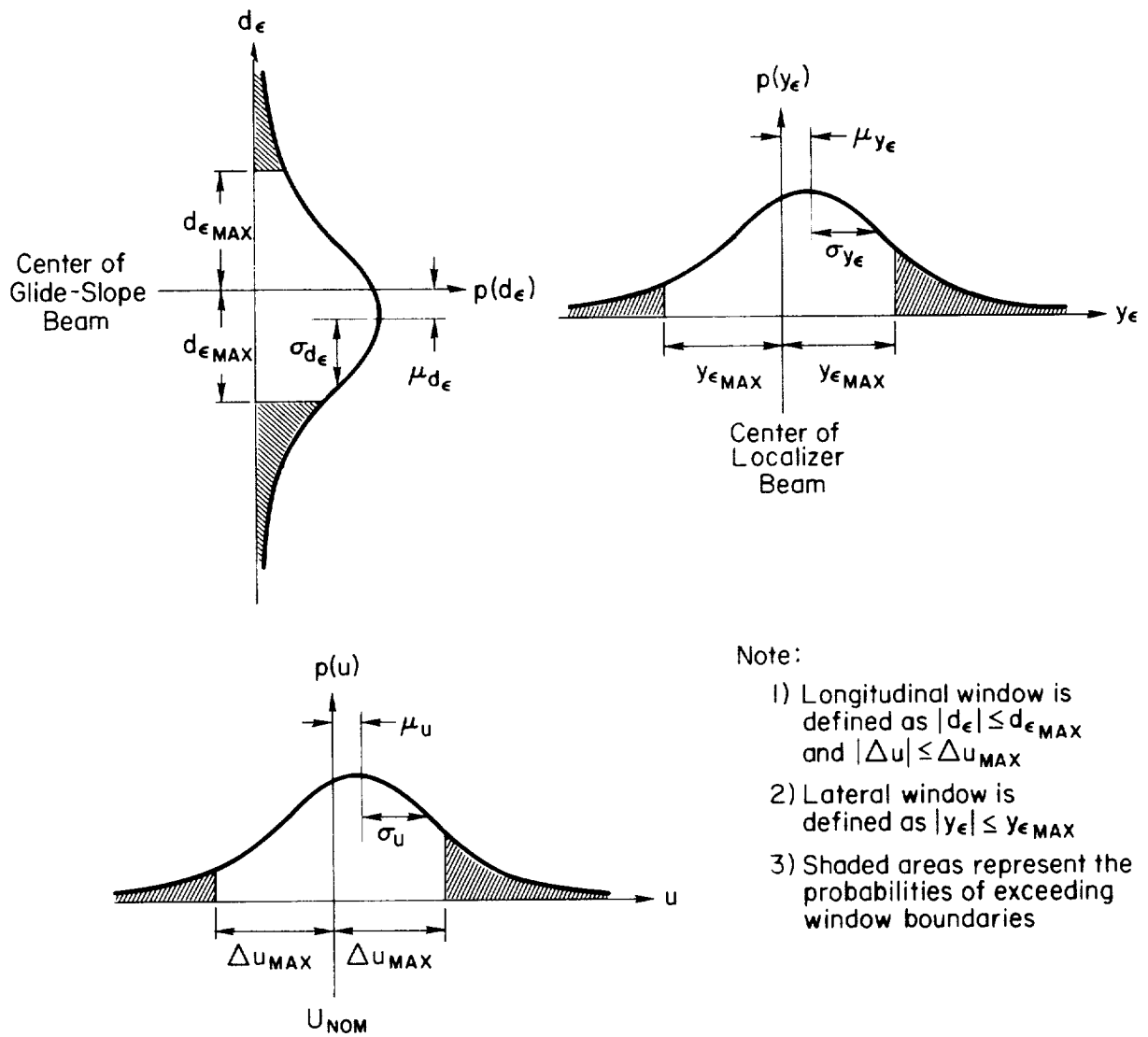
Figure 25. Probability Density Distributions for Deviations from the Glide Slope Beam, Localizer Beam, and Nominal Velocity

The probability of being outside of the longitudinal window is a little more complicated in that it involves altitude $\underline{\text{and}}$ airspeed deviations.

$$P_{\text{out-long}} = F\left(\frac{12 \text{ ft} + \mu_{d_\epsilon}}{\sigma_{d_\epsilon}}\right) + F\left(\frac{12 \text{ ft} - \mu_{d_\epsilon}}{\sigma_{d_\epsilon}}\right) + F\left(\frac{5 \text{ kts} + \mu_u}{\sigma_u}\right) + F\left(\frac{5 \text{ kts} - \mu_u}{\sigma_u}\right)$$

$$- \left[F\left(\frac{12 + \mu_{d_\epsilon}}{\sigma_{d_\epsilon}}\right) + F\left(\frac{12 - \mu_{d_\epsilon}}{\sigma_{d_\epsilon}}\right)\right]\left[F\left(\frac{5 + \mu_u}{\sigma_u}\right) + F\left(\frac{5 - \mu_u}{\sigma_u}\right)\right] \quad (17)$$

Now all that remains to define the combined probability of a successful Category II approach is to combine the above results. Thus, assuming that longitudinal and lateral deviations are independent,

$$P_{\text{MA}_{\text{total}}} = P_{\text{out-long}} + P_{\text{out-lat}}(1 - P_{\text{out-long}}) \quad (18)$$

and

$$P_{\text{successful approach}} = 1 - P_{\text{MA}_{\text{total}}} \quad (19)$$

$$= (P_{\text{SA-long}})(P_{\text{SA-lat}})$$

In the next section the calculation of the various μ's and σ's will be discussed and some example calculations will be presented.

SECTION V

EXAMPLE CALCULATIONS

From Section IV it was found that the quantities required to compute the desired probabilities are the means and rms deviations from the means for certain of the variables. Fortunately, the calculations of these means and rms deviations are quite simple to perform. The mean values of the variables are computed from deterministic inputs, and the rms values from zero-mean Gaussian* (random) inputs, as indicated schematically in Fig. 26.
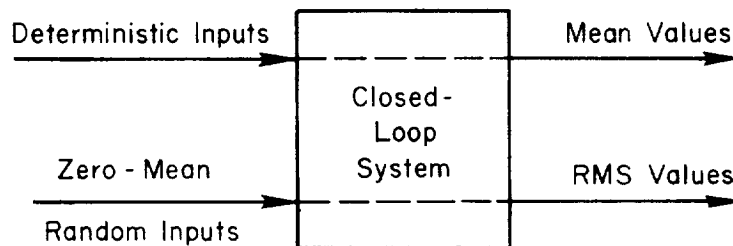
Figure 26. Schematic Representation of Effects
of Deterministic and Random Inputs

The deterministic inputs are easily handled via either a digital or analog computer (where the inputs are applied to the system as functions of time, and time histories of the pertinent variables are recorded). The value of each variable at the decision height is a number. These numbers are, by definition, the means of these quantities at the decision height. Clearly, if there are no deterministic inputs, then the mean for each variable is zero.

---

*It is noted that Gaussian inputs applied to a linear system will produce Gaussian outputs for each variable. Further, the rms value of each output will be directly proportional to the rms value of the input (for a single input). For several independent inputs, the rms value of each output is the square root of the sum of the squares of the rms values due to each input.

A digital computer is used to compute the rms values for Gaussian inputs. The inputs are entered in the form of filtered white noise (with the filters determined by the input power spectra). The computer program then gives the rms values as outputs. If there are no random inputs, then the rms deviation from the mean for each variable is clearly zero. Thus, you get a σ from zero-mean random inputs, and a mean from deterministic inputs. Therefore, for a linear system, a combination of deterministic and random inputs gives a mean _and_ a σ for each variable.

Four longitudinal examples and one lateral example will be presented to indicate how system comparisons can actually be made, as well as to clarify the procedures involved. For this purpose a DC-8 airplane was selected. Of the four longitudinal systems, three are automatic and one is a manually controlled flight director. All of the systems are briefly described in Appendix B. The three automatic longitudinal systems are designated as Systems A, B, and C. (For easy reference, System A represents an advanced system, and System C represents a more conventional system. System B represents a system that is more sophisticated than C, but less than A.) The automatic longitudinal system examples will be presented first.

For the first example, the inputs will be random gusts for u_g and w_g, and Gaussian glide slope beam noise. Using the closed-loop transfer functions for d_ϵ (deviation from the glide slope beam) and u to "d" commands and gust inputs, the rms values of d_ϵ and u for unit gust inputs (i.e., 1 ft/sec rms) and the total beam noise are determined via Eqs. 20 through 25. Note that new symbols are defined in these equations to simplify the writing of subsequent equations.

$$\sigma_{d_1}^2 \equiv \left(\frac{\sigma_{\hat{d}_\epsilon}}{\sigma_{w_g}}\right)^2 = \int_0^\infty \left|\left(\frac{\hat{d}_\epsilon}{w_g}\right)_{\text{closed loop}}\right|^2 \frac{\Phi_{w_g}(\omega)}{\sigma_{w_g}^2} \, d\omega \qquad (20)$$

$$\sigma_{d_2}^2 \equiv \left(\frac{\sigma_{\hat{d}_\epsilon}}{\sigma_{u_g}}\right)^2 = \int_0^\infty \left|\left(\frac{\hat{d}_\epsilon}{u_g}\right)_{\text{closed loop}}\right|^2 \frac{\Phi_{u_g}(\omega)}{\sigma_{u_g}^2} \, d\omega \qquad (21)$$

$$\sigma_{d_{gs}}^2 \equiv \int_0^\infty \left|\left(\frac{\hat{d}_\epsilon}{d_{command}}\right)_{closed\ loop}\right|^2 \Phi_{glide\ slope\atop noise}(\omega)\ d\omega \tag{22}$$

$$\sigma_{u_1}^2 \equiv \left(\frac{\sigma_u}{\sigma_{w_g}}\right)^2 = \int_0^\infty \left|\left(\frac{u}{w_g}\right)_{closed\ loop}\right|^2 \frac{\Phi_{w_g}(\omega)}{\sigma_{w_g}^2}\ d\omega \tag{23}$$

$$\sigma_{u_2}^2 \equiv \left(\frac{\sigma_u}{\sigma_{u_g}}\right)^2 = \int_0^\infty \left|\left(\frac{u}{u_g}\right)_{closed\ loop}\right|^2 \frac{\Phi_{u_g}(\omega)}{\sigma_{u_g}^2}\ d\omega \tag{24}$$

$$\sigma_{u_{gs}}^2 \equiv \int_0^\infty \left|\left(\frac{u}{d_{command}}\right)_{closed\ loop}\right|^2 \Phi_{glide\ slope\atop noise}(\omega)\ d\omega \tag{25}$$

The results of these computations are summarized in Table IX for the "primary" system (A), and for the other two automatic systems as well. It is noted that the values given in the table can be used directly to compare the relative merits of the three systems. Although it is not the

TABLE IX

SUMMARY OF LONGITUDINAL RMS VALUES FOR SEVERAL INPUTS

SYMBOL	DEFINITION	MAGNITUDE			UNITS
		SYSTEM A	SYSTEM B	SYSTEM C	
σ_{d_1}	$\sigma_{\hat{d}_\epsilon}$ due to $\sigma_{w_g} = 1$ ft/sec	0.5660	1.0627	1.1377	ft
σ_{d_2}	$\sigma_{\hat{d}_\epsilon}$ due to $\sigma_{u_g} = 1$ ft/sec	0.4410	1.3032	1.1543	ft
$\sigma_{d_{gs}}$	$\sigma_{\hat{d}_\epsilon}$ due to glide slope noise (10 μa rms)	1.6465	1.6850	1.4423	ft
σ_{u_1}	σ_u due to $\sigma_{w_g} = 1$ ft/sec	0.3574	0.3547	0.3088	ft/sec
σ_{u_2}	σ_u due to $\sigma_{u_g} = 1$ ft/sec	0.3045	0.3578	0.3498	ft/sec
$\sigma_{u_{gs}}$	σ_u due to glide slope noise (10 μa rms)	0.2406	0.2115	0.1714	ft/sec

intent here to compare systems on such a basis, Figs. 27, 28, and 29 are examples of how such a comparison can be made graphically (using the numbers from Table IX). This particular comparison is made on the basis of random u_g, w_g, and glide slope noise applied individually to each system. In these three figures, parameters other than just σ_u and σ_{d_ϵ} are given for completeness. Several comments can be made concerning this comparison. First, System A is seen to be considerably better than the other two systems on the basis of σ_{d_ϵ} (although at the expense of larger σ_w, σ_Δ, and σ_{δ_e} — but this is expected because System A has a higher bandwidth). Second, on the basis of σ_u all three systems are about the same. This is because no considerations of speed control were made in deriving any of the loop closures. Thus, each system exhibits essentially the basic speed characteristics of the bare airframe. Further, it is noted that for these random type inputs applied to Systems B and C the magnitude of σ_{d_ϵ}, expressed as a fraction of $d_{\epsilon_{max}}$, is a lot larger than σ_u expressed as a fraction of u_{max}. This means that the probabilities of missed approaches for Systems B and C are almost entirely due to d-excursions, and have only an insignificant contribution from speed variations. This is a particularly interesting result, considering that no speed loop was closed! Thus the fact that Systems B and C are considerably inferior to System A on a successful approach probability basis is a direct result of the larger d-excursions of Systems B and C, along with the fact that d-excursions (and not u-excursions) produce most of the missed approaches for B and C.

Getting back to the step by step presentation of the technique for computing probabilities, the "total" rms values of d_ϵ and u are found from,

$$\sigma_{\hat{d}_\epsilon} = \sqrt{\sigma_{d_1}^2 \sigma_{w_g}^2 + \sigma_{d_2}^2 \sigma_{u_g}^2 + \sigma_{d_{gs}}^2} \qquad (26)$$

and,

$$\sigma_u = \sqrt{\sigma_{u_1}^2 \sigma_{w_g}^2 + \sigma_{u_2}^2 \sigma_{u_g}^2 + \sigma_{u_{gs}}^2} \qquad (27)$$

Equations 26 and 27 can be simplified by making use of the relation between σ_{w_g} and σ_{u_g} given in Section III for an altitude of 100 ft. That is,

$$\sigma_{u_g} = 2.59 \sigma_{w_g} \qquad (28)$$
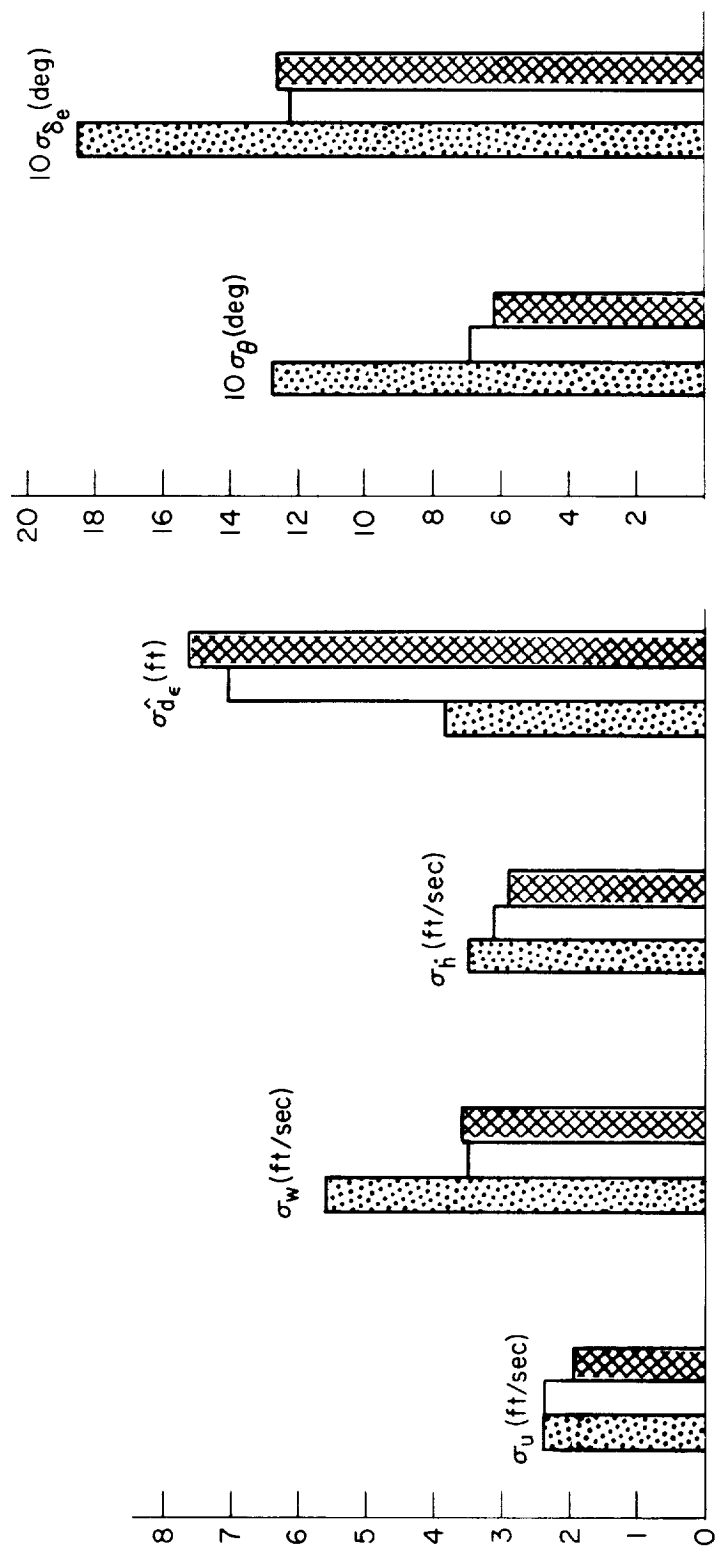
Figure 27. σ-Values for Random w_g Input of Approximately 4 kts RMS
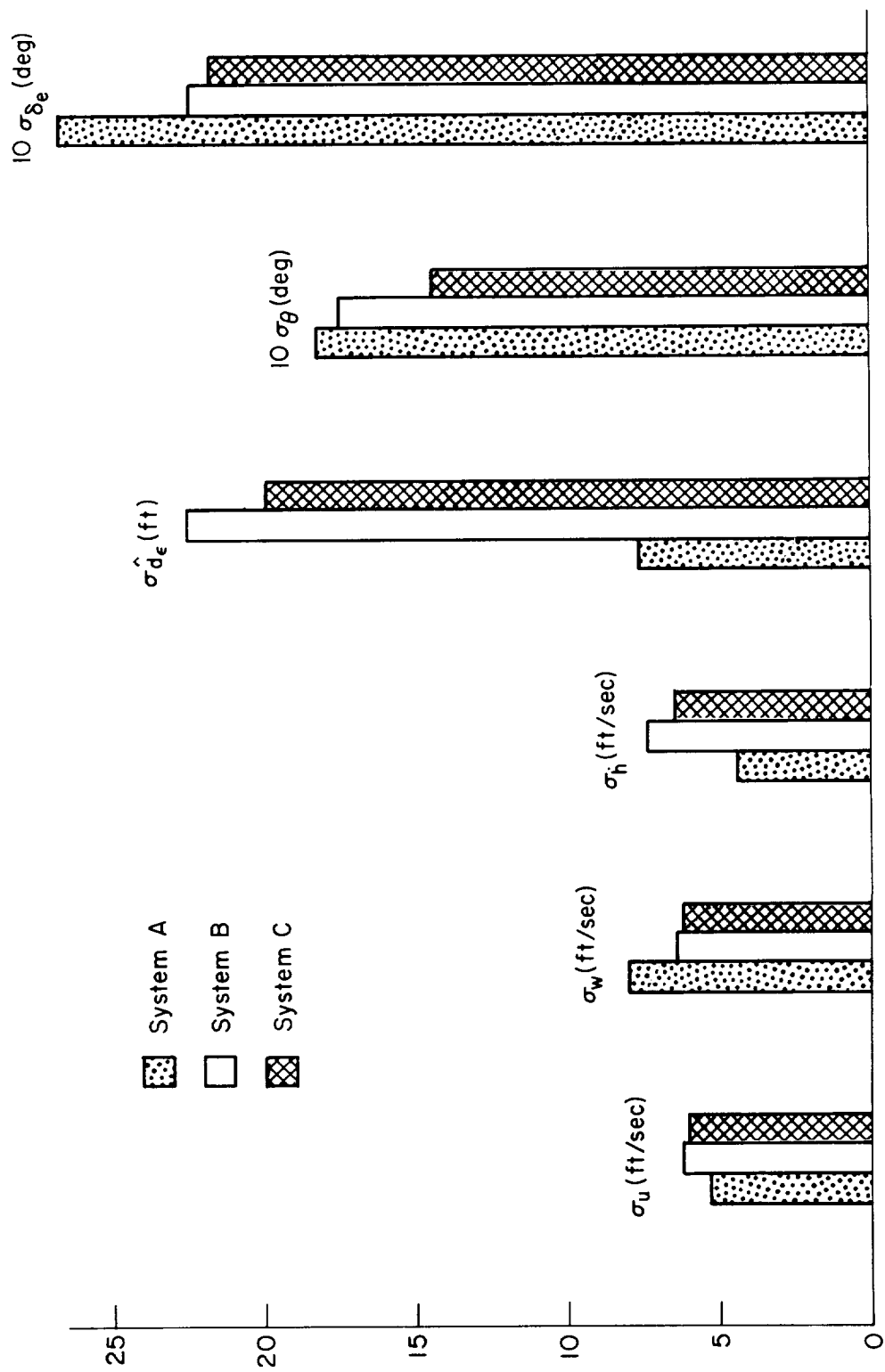
Figure 28. σ-Values for Random u_g Input of Approximately 10 kts RMS
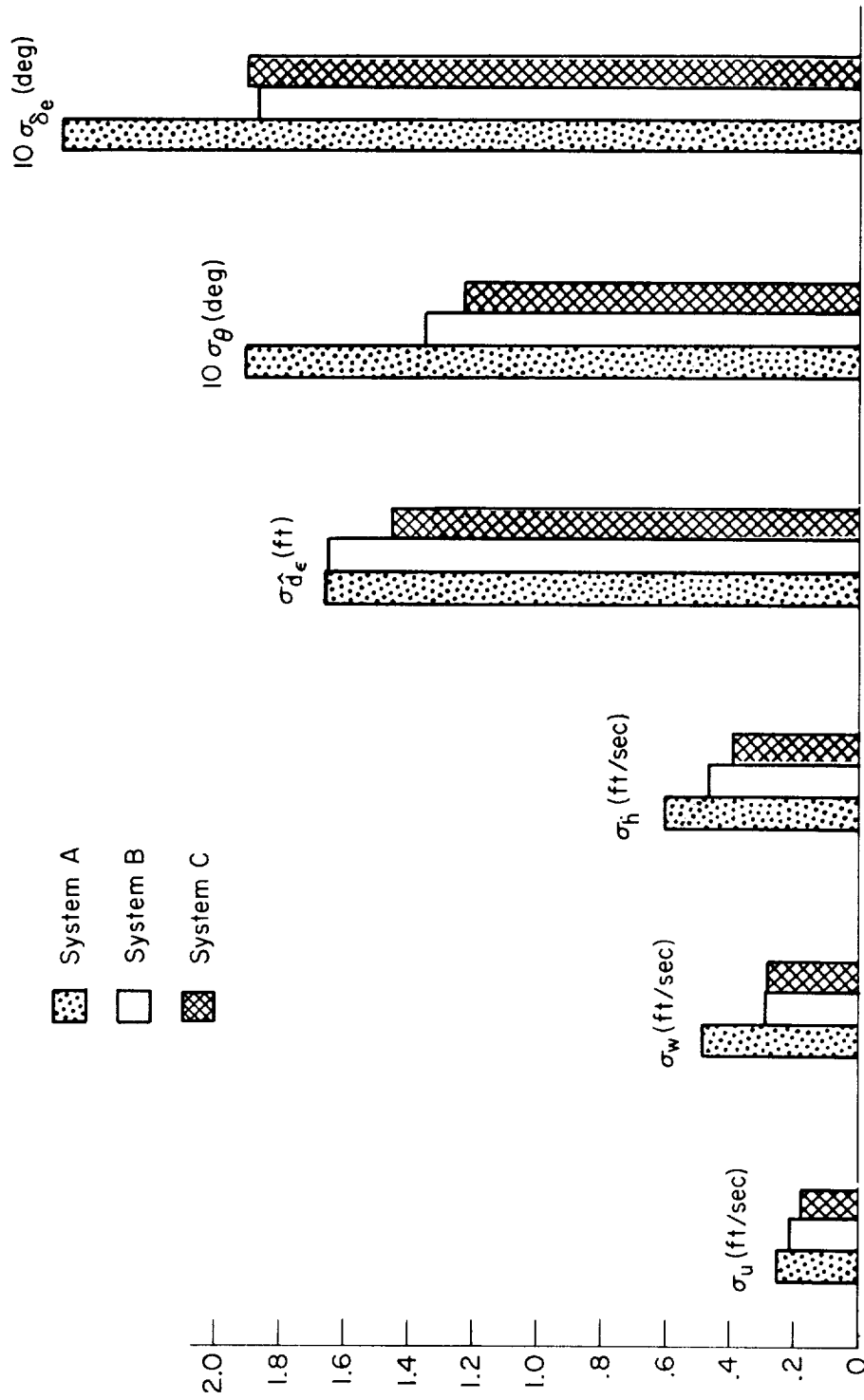
Figure 29. σ-Values for Glide Slope Noise of 10 μa RMS (Approximately 1.7 ft RMS) at 100 ft Altitude

Thus, using Eq. 28 and the values in Table IX for System A, Eqs. 26 and 27 become,

$$\sigma_{\hat{d}_\epsilon}(ft) = \sqrt{1.62\sigma_{w_g}^2 + 2.71} \qquad (29)$$

$$\sigma_u(ft/sec) = \sqrt{0.750\sigma_{w_g}^2 + 0.058} \qquad (30)$$

Figure 30 is a plot of these last two relations (for System A), and shows that the glide slope noise contribution is negligible for σ_{w_g} greater than about 2 ft/sec.

At this point we could pick a value for σ_{w_g} (for example, the value that is exceeded 1 percent of the time) and obtain values for σ_{d_ϵ} and σ_u. These values could then be substituted into the equations given in Section IV to compute the probability of a longitudinal missed approach. In fact, several values of σ_{w_g} could be selected and the probability of a successful longitudinal approach ($P_{SA} = 1 - P_{MA}$) could be plotted as a function of σ_{w_g}. Such a plot is presented in Fig. 31 for System A, where it can be seen that the probability of a successful longitudinal approach drops below 0.5 when σ_{w_g} exceeds about 9 ft/sec.

Similar probabilities could be computed for alternative systems, and comparisons could be made. However, these probabilities are conditional probabilities (because they are based on the assumption of a given gust level) and bear no relation to the actual longitudinal missed-approach probability, except when the wind conditions are as assumed. Therefore, a further sophistication will be introduced here to account for the distribution of gust levels. This will enable an "overall" probability of a longitudinal successful approach to be made — one that will be more meaningful in terms of long-time nationwide averages.

This overall probability is preferred over the conditional probability as a performance metric for comparison of systems because it makes possible a quantitative assessment of relative system merit. That is, a dollars-and-cents value of one system over another can be made if an overall approach success probability is known — as opposed to only knowing
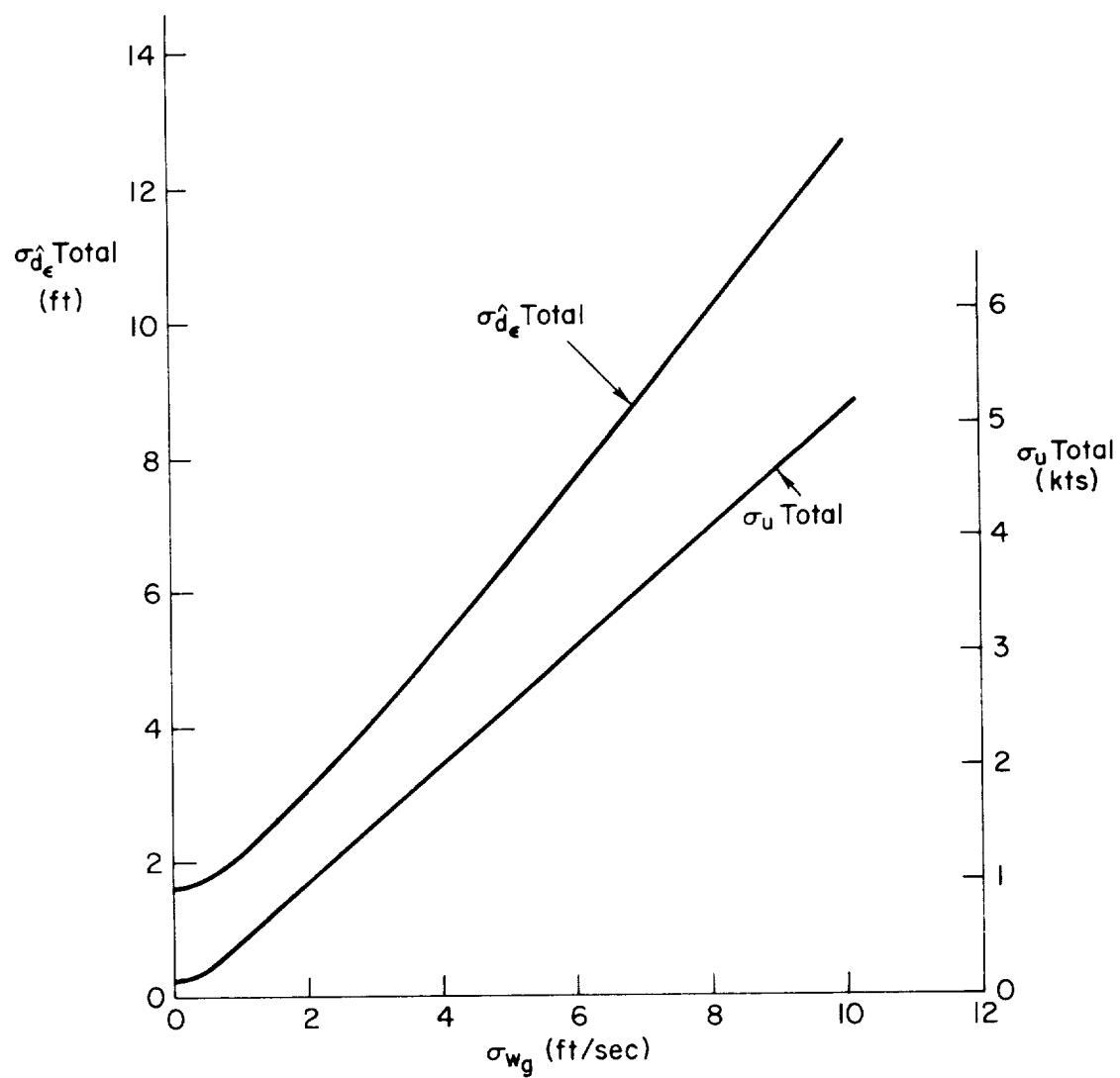
Figure 30. $\sigma_{\hat{d}}$ (Total) and σ_u(Total) as Function of the w_g Gust Intensity
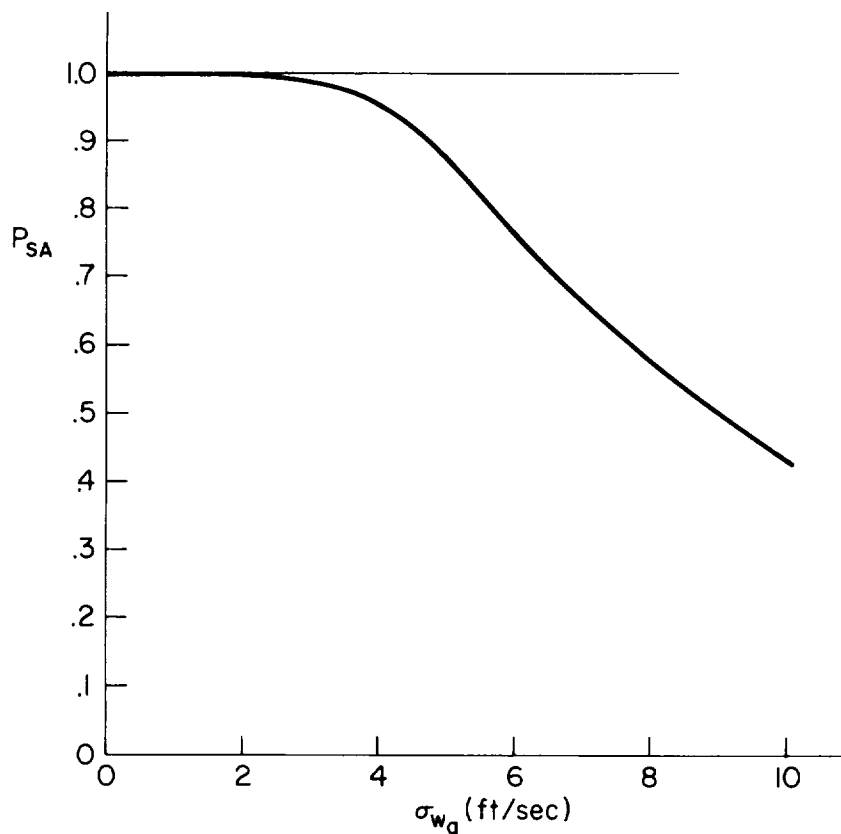
Figure 31. Probability of a Successful Longitudinal Approach
as a Function of the w_g Gust Intensity (System A)

that one system will result in 10 percent more missed approaches than another when σ_{w_g} is 5 ft/sec, and 17 percent more missed approaches when σ_{w_g} is 3 ft/sec. The key point here is that the _ratio_ (as well as the difference) of missed approach probabilities for two different systems is a function of the gust level encountered. Therefore, the relative value of one system over another will depend on the gust level encountered. This is not to say that a probability calculation made on the basis of a given gust level is of no use, because it is easy to conceive of a situation in which the decision to fly to an alternate field is made _prior_ to arriving at the primary destination on the basis of a very high gust level at the primary destination— and its associated low probability of a successful approach. What we are saying is that _system comparisons_

should be made on the basis of _overall_ probabilities in order to make differences between systems assessable in meaningful terms.

The manner in which the distribution of gust levels is taken into consideration is seen in Eq. 31,

$$P_{MA} = 0.2P(MA|\sigma_{w_g} = 0) + 0.8 \int_0^\infty P(MA|\sigma_{w_g})p(\sigma_{w_g})d\sigma_{w_g} \tag{31}$$

where P_{MA} is the overall probability of a missed approach

$P(MA|\sigma_{w_g})$ is the conditional probability of a missed approach; and is a function of σ_{w_g} (see discussion leading to Fig. 21)

$p(\sigma_{w_g})$ is the probability density distribution of σ_{w_g}, given that clear air turbulence is encountered (see next paragraph)

0.8 is the probability of encountering clear air turbulence at an altitude of 100 ft (see Section III)

The function $p(\sigma_{w_g})$ is determined from $\hat{P}(\sigma_{w_g})$, given in Section III, by differentiation. Thus,

$$p(\sigma_{w_g}) = \frac{\sigma_{w_g}}{5.29} e^{-(1/2)(\sigma_{w_g}/2.3)^2} \tag{32}$$

With this last equation it is now a simple matter to compute the overall probability of a missed approach (or a successful approach). It can be done by hand calculations in a few hours, or via a simple digital computer program in a few minutes. For the example case of System A with random u_{gust}, w_{gust}, and glide slope noise, the overall probability of a successful longitudinal approach is 0.976. However, by adding a u_{gust} wind shear of 4 kt per 100 ft from 200 ft to 100 ft the probability drops to 0.90. (Wind shear was found to be the most critical deterministic input.) These numbers come from Table X which shows a comparison of longitudinal approach success probabilities for two sets of inputs applied to the three example automatic systems. Also

TABLE X

LONGITUDINAL APPROACH SUCCESS PROBABILITIES FOR THE AUTOMATIC SYSTEMS

SYSTEM	RANDOM u_g AND w_g AND GLIDE SLOPE NOISE		RANDOM u_g AND w_g, GLIDE SLOPE NOISE AND u_g SHEAR = 4 KT/100 FT FOR LAST 100 FT BEFORE WINDOW	
	Longitudinal P_{SA} for σ_{w_g} = 4 ft/sec*	OVERALL LONGITUDINAL P_{SA}	Longitudinal P_{SA} for σ_{w_g} = 4 ft/sec*	OVERALL LONGITUDINAL P_{SA}
A	0.965	0.976	0.78	0.90
B	0.58	0.80	0.46	0.71
C	0.63	0.83	0.49	0.74

*This gust level occurs about 18 percent of the time (Ref. 2).

included in the table is a column giving the probability of a successful longitudinal approach for a gust level that is equalled or exceeded about 18 percent of the time. This column was presented to show that the missed-approach rate for a moderately gusty condition is considerably greater than the overall average missed-approach rate.

This brings up an interesting point. One may wonder if there is a single gust level that can be considered representative, in that it gives the same probability as does the overall integrated gust distribution. For any given system the answer is obviously yes. But as a practical mat-ter the answer is unfortunately no. The single gust level that gives the same probability as the overall integrated gusts for System A doesn't work for System C, and vice versa. The problem is that the relations among rms values, mean values, and probabilities are very nonlinear. Consequently, probabilities don't scale with input disturbances. As a result, every time the system or an input (e.g., shear) is changed, a new "equivalent" gust level must be found.

A comparison of the approach success probabilities in Table X shows that System A is considerably better than either B or C, and that C is slightly better than B. System A's clear superiority was certainly no

surprise. In fact, it was an expected result because System A was designed
to be an "advanced" longitudinal autopilot — optimized for the given air-
plane dynamics. Systems B and C represent more modest autopilots (although
the gains were optimized for the given airplane). However, the result
showing System C to be better than B might be considered somewhat of a
surprise because time traces of the "d" and "u" responses to u_g and w_g
step inputs (given in Ref. 12) show System B to be slightly superior to C.
On examining these time traces, it is found that the $\dot{h}$ response to these
step gust inputs indicates a slight advantage of System C over B. The
significance of this is explained as follows. First, the d response to a
step gust is clearly indicative of the step response of a system. Next,
the $\dot{h}$ response to a step gust can be used to approximate the $\dot{d}$ response
to a step gust. But the $\dot{d}$ response to a step gust is the same as the d
response to a gust impulse. Thus the $\dot{h}$ response to a step gust is indica-
tive of the d response to a gust impulse. The net result is that System B
is slightly superior to C for step gust inputs, but is slightly inferior
to C for impulsive gust inputs. Because the response to a random gust
input more closely resembles that from an impulsive-type input than that
from a step-type input, the probability of a successful approach (with
the random gust input) favored System C by a small amount. However,
because the two systems are so similar, the determination of the better
system surely must be made on the basis of a more comprehensive comparison
than just a random gust input disturbance. If a step w_{gust} input had
been used, System B would have been found to be clearly superior to C.
System B would also be found to be superior for a pitch attitude bias
input. Thus it is fully recognized that the above result favoring System
C is only one of several criteria for judging the relative merits of com-
peting systems. In addition to subjecting the system models to other
inputs, such factors as reliability, maintainability, etc., must also be
considered.

At this point it seems that a lesson can be learned from the above
discussion comparing Systems B and C. This is that one must not be blinded
by preconceived notions of what is good and what is not so good. If, in
fact, the input that showed System C to be superior to B is encountered
regularly, then it may be the pertinent metric to use in comparing the two

systems. In other words, one must not judge too hastily; a system may have many advantages over an alternative system, but it may be inferior in the one category that counts most.

To demonstrate the applicability of the approach model to a human-pilot situation, the approach success probabilities for a manually controlled flight director approach (in the same DC-8) will be presented next.

The mechanization of the flight director, as well as estimates for the pilot's describing function and remnant, are required to define the manual system. These items are described in Appendix B. A key point in the analysis technique is that once these elements of the system are known (or estimated), the analytical procedures are identical to those for an automatic system. As a result, the manual example would involve just a repeat of the prior calculations with new numbers. Because this would not help in clarifying the use of the approach model, only the resulting probabilities will be presented here (to enable comparison with the automatic systems). Table XI shows the longitudinal approach success probabilities for the manually controlled flight director system with and without the estimated remnant. It is seen that the effect of the remnant is small (compared to the effect of the random gusts) as far as the approach success probability is concerned. This is a consequence of the assumption that the remnant scales with the displayed error (see Appendix B). When the error is large there are missed approaches regardless of the remnant, and when the error is small the remnant contribution is also small. The

TABLE XI

LONGITUDINAL APPROACH SUCCESS PROBABILITIES FOR THE
MANUALLY CONTROLLED FLIGHT DIRECTOR SYSTEM

RANDOM u_g AND w_g AND GLIDE SLOPE NOISE		RANDOM u_g AND w_g, GLIDE SLOPE NOISE, AND REMNANT	
LONGITUDINAL P_{SA} FOR $\sigma_{w_g} = 4$ ft/sec[*]	OVERALL LONGITUDINAL P_{SA}	LONGITUDINAL P_{SA} FOR $\sigma_{w_g} = 4$ ft/sec[*]	OVERALL LONGITUDINAL P_{SA}
0.63	0.83	0.60	0.81

[*]This gust level occurs about 18 percent of the time (Ref. 2).

61

net effect is that the remnant is not a very significant contributor to missed approaches.

To complete the calculation of a combined overall missed approach probability, a lateral example is presented next. Because the analytical technique is again the same as that used for the longitudinal calculations, it is again unnecessary to repeat the computational details. Therefore, only the major points of the lateral example will be presented. A brief description of the lateral airplane dynamics and example control system is included in Appendix B.

Localizer noise and random gusts for v_g and p_g were used as disturbance inputs. Because the rms level of the gust components at any given altitude are related as shown in Eq. 9, it is convenient for comparison purposes to continue to express the gust level by the value of σ_{w_g}. For the lateral situation the only window constraint is the deviation from the center of the localizer beam. Figure 32 shows the total rms lateral dispersion (due to v_g, p_g, and localizer noise) as a function of the σ_{w_g} level. It is seen that the rms dispersions are a much smaller fraction of the window limit than was the case for the longitudinal situation. Figure 33 then shows the probability of a successful lateral approach as a function of the σ_{w_g} level. For corresponding gust levels it is seen that the probability of a successful lateral approach is considerably higher than that for a successful longitudinal approach (see Fig. 31). By integrating over all gust levels, the overall probability of a successful lateral approach is found to be 0.9987. The addition of a lateral wind shear of 8 kts per 100 ft from 200 ft down to 100 ft would give a lateral offset at the window of 14 ft. When the random gusts and localizer noise are superimposed on this shear the probability of a successful lateral approach is lowered to 0.9975. These probabilities are summarized in Table XII, which is the lateral counterpart to Table X. Finally, when the lateral system is combined with each of the three longitudinal systems, the overall probability of a successful approach can be computed for each combination. These results are given in Table XIII.

The above examples show the usefulness of the model as presented herein. It provides a practical means for comparing systems (on the basis
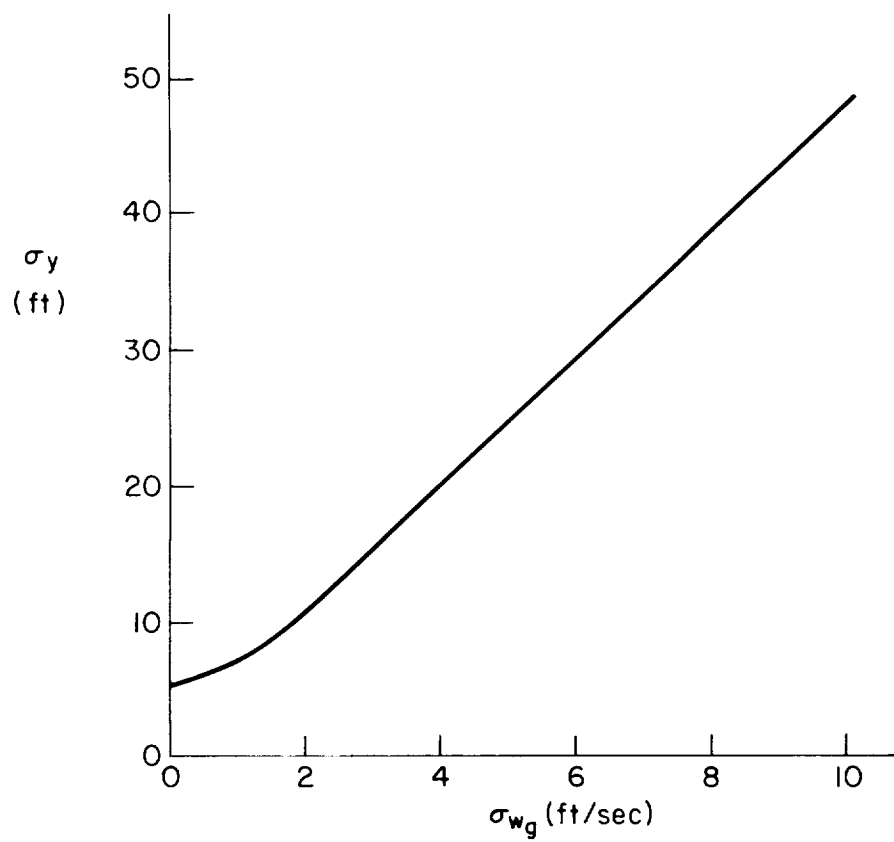
Figure 32. $\sigma_y(\text{Total})$ as a Function of the w_g Gust Intensity
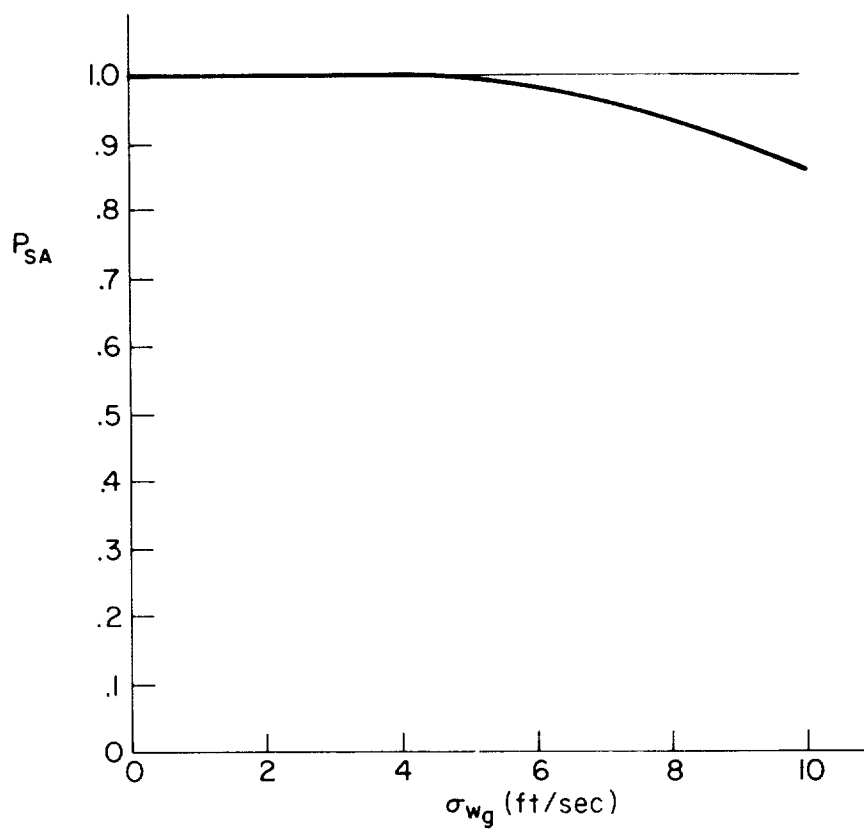
Figure 33. Probability of a Successful Lateral Approach
as a Function of the w_g Gust Intensity

TABLE XII

LATERAL APPROACH SUCCESS PROBABILITIES

RANDOM v_g AND p_g AND LOCALIZER NOISE		RANDOM v_g AND p_g, LOCALIZER NOISE AND v_g SHEAR = 8 KT/100 FT FOR LAST 100 FT BEFORE WINDOW	
LATERAL P_{SA} FOR σ_{w_g} = 4 FT/SEC*	OVERALL LATERAL P_{SA}	LATERAL P_{SA} FOR σ_{w_g} = 4 FT/SEC*	OVERALL LATERAL P_{SA}
0.9997	0.9987	0.9982	0.9975

*This gust level occurs about 18 percent of the time (Ref. 2).

TABLE XIII

COMBINED (LONGITUDINAL AND LATERAL)
APPROACH SUCCESS PROBABILITIES

LONGITUDINAL SYSTEM	RANDOM u_g, v_g, w_g, AND GLIDE SLOPE AND LOCALIZER NOISE		RANDOM u_g, v_g, w_g, GLIDE SLOPE AND LOCALIZER NOISE, u_g SHEAR = 4 KT/100 FT AND v_g SHEAR = 8 KT/100 FT FOR LAST 100 FT BEFORE WINDOW	
	P_{SA} FOR σ_{w_g} = 4 FT/SEC*	OVERALL P_{SA}	P_{SA} FOR σ_{w_g} = 4 FT/SEC*	OVERALL P_{SA}
A	0.965	0.975	0.78	0.90
B	0.58	0.80	0.46	0.71
C	0.63	0.83	0.49	0.74

*This gust level occurs about 18 percent of the time (Ref. 2).

of approach success probabilities), rather than an "academic" means (as would be the case if all of the various aspects of each system were not combined to assess the critical performance parameter — or parameters).

It is pertinent here to make a few comments concerning the effect of a nonzero mean on the probability calculations. As an example, Fig. 34 shows the effect of a nonzero mean on the probability of landing off the side of the runway. (This example was chosen for ease of visualization.)

65
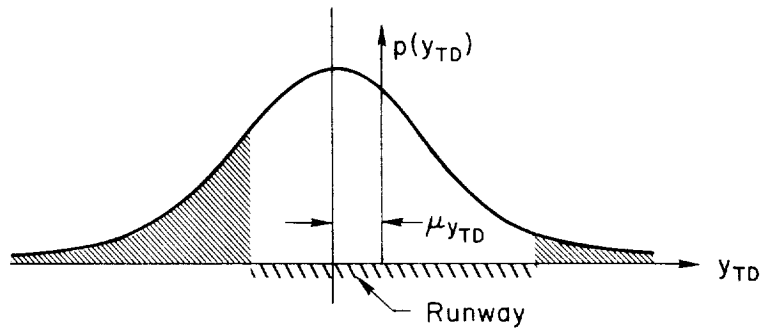
Figure 34. Effect of Nonzero Mean on the Probability of Landing
Off the Side of a Runway (Represented by shaded area)

It is seen that the area under the right-hand tail is diminished, and the
area under the left-hand tail is increased due to the mean being to the
left of the center of the runway. The important point here is that the
decrease in area on the right-hand tail is much less than the increase
in the area on the left-hand tail. In fact, it is generally true that
when the mean moves very far from zero, the area under one tail becomes
so large compared to the area under the other one that the smaller tail
can be neglected. The significance of this is that when shear-type inputs
(and others which give a nonzero mean) are combined with random inputs
the probability of landing off the side of the runway, for example, becomes
quite large compared to the probability of landing off the side of the run-
way when only zero-mean Gaussian-type inputs are considered. (This same
situation can exist with the other types of accidents, such as long landing
short landings, hard landings, etc., as well as for the situation at the
approach window, where the parameter of interest is the probability of an
approach success.) Thus, since zero-mean random gusts are present most of
the time, a relatively high percentage of those occasions when shears
(for example) are encountered will result in missed approaches (or acci-
dents). Conversely, few missed approaches (or accidents) will occur when
shears are not present.

SECTION VI

SUMMARY AND CONCLUSIONS

In this report we have confined our attention to the final approach phase of flight, from glide slope acquisition down to the Category II decision height of 100 ft. During this phase the primary tasks are glide slope and localizer tracking, while the pertinent disturbance inputs are random and discrete gusts and beam noise (bends). The controllers used in the examples included fully automatic systems, as well as a manual flight director system. Further, the example calculations included both the longitudinal and lateral situations.

With the above "components" of the approach system model it is possible to compute performance metrics. The key feature in this report is that we have derived an analytical expression for the overall approach success probability that is sensitive to changes in the basic airframe, the controller logic and mechanization, the displays used, types of inputs considered, and the dimensions of the approach window at the decision height. Thus, competing airframes, control systems, or displays (e.g., flight directors) can be compared directly. The model has a further capability in that the effects of changes in the approach window can easily be assessed.

The numerical examples presented in Section V showed the effects of changes in feedback loops and equalization on the probability of a successful approach for a DC-8 type airplane. The example exercises showed quantitatively that a combination of inputs, such as wind shears and random gusts, leads to a significantly higher missed approach rate than would exist with either input by itself. The examples also showed that beam bends do not play a significant role in producing missed approaches. Further, an overwhelming majority of Category II missed approaches would be the result of altitude dispersions (as compared to those resulting from lateral position dispersions) for the advanced automatic system (System A) in a DC-8.

REFERENCES

1. Wood, K. A., "The Calculation of Weather Minima — Part I — RVR Minima," All-Weather Operations Panel, Third Meeting, Volume II, Selected Working Papers, International Civil Aviation Organization Doc. No. 8685, AWOP/III-2, 1967, pp. 167-185.

2. Johnson, W. A. and D. T. McRuer, "A System Model for Low Level Approach," AIAA Guidance, Control and Flight Mechanics Conference, Santa Barbara, California, August 17-19, 1970, AIAA Paper No. 70-1034.

3. Durand, Tulvio S., and Gary L. Teper, An Analysis of Terminal Flight Path Control in Carrier Landing, Systems Technology, Inc., Tech. Rept. 137-1(R), Aug. 1964.

4. Private Pilot's Handbook of Aeronautical Knowledge, Federal Aviation Agency, Flight Standards Service, July 1963.

5. Crossley, A. F., and J. A. Harker, Vertical Shear in the Lower Layers at Cardington, Beds, Air Ministry, Meteorological Office I.D.M. 101, 1967.

6. Kramer, K. C., "Category II Operation — No Performance Compromise," Second International Aviation Research and Development Symposium, Atlantic City, New Jersey, 16-18 Sept. 1963.

7. McRuer, Duane, Irving Ashkenas, and Dunstan Graham, Aircraft Dynamics and Automatic Control, Princeton University Press, 1972.

8. Armitage, H. B., "A Pilot's Evaluation of the C-141 Category IIIb All Weather Landing System," Society of Experimental Test Pilots, Technical Review, Vol. 9, No. 3, 1969, pp. 61-77.

9. Snyder, C. Thomas, Analog Study of the Longitudinal Response of a Swept-Wing Transport Airplane to Wind Shear and Sustained Gusts During Landing Approach, NASA TN D-4477, Apr. 1968.

10. Weir, David H., and Richard H. Klein, The Measurement and Analysis of Pilot Scanning and Control Behavior During Simulated Instrument Approaches, NASA CR-1535, June 1970.

11. Criteria for Approval of Category II Landing Weather Minima, FAA AC No. 120-20, 6 June 1966.

12. McRuer, D. T., and W. A. Johnson, Development of Approach Control System Requirements with Applications to a Jet Transport, Systems Technology, Inc., Tech. Rept. 182-3, Oct. 1970. NASA CR-2023.

13. Weir, D. H., R. H. Klein, and D. T. McRuer, <u>Principles for the Design of Advanced Flight Director Systems Based on the Theory of Manual Control Displays</u>, Systems Technology, Inc., Tech. Rept. 170-5, Mar. 1970. (Forthcoming NASA CR-)

14. McRuer, Duane, Dunstan Graham, Ezra Krendel, and William Reisener, Jr., <u>Human Pilot Dynamics in Compensatory Systems — Theory, Models, and Experiments with Controlled Element and Forcing Function Variations</u>, AFFDL-TR-65-15, July 1965.

APPENDIX A

ACCIDENT AND INCIDENT STATISTICS

The air carrier terminal area accident and incident statistics for 1964, 1965, and 1966 are presented in this appendix. This information can be used to validate certain aspects of the approach model, as well as to point out aspects of approach and landing that deserve further study.

The necessary data for validation of the model consists of

- Number of air carrier operations
- Number of air carrier instrument approaches
- Number of air carrier incidents which are takeoff- or landing-related
- Number of air carrier accidents which are takeoff- or landing-related

for a given interval of time. In the latter two sets of data it is also necessary to distinguish between landing incidents/accidents which occur from factors originating during instrument flight in distinction to visual flight. Further breakdown into type of incident/accident, type of aircraft, etc., is helpful for confirming finer grain structure of the model.

The numerical data referred to above is used for constructing the probabilities for occurrence of different types of incidents/accidents. The basis, or population, used for calculating these probabilities is one-half the number of air carrier operations, or the number of air carrier instrument approaches, as is appropriate. (Numbers are given in Tables A-I and A-II for each of three relatively recent years for which complete and consistent data are available.) Notice that probabilities are therefore on a per-takeoff, -landing, or -instrument approach landing basis, which is directly applicable for terminal operations study. If required, these statistics can be tied in with many of the better-known (but here inappropriate) statistics based upon passenger-miles, flight hours, or whatever, by researching appropriate conversion factors. Of course, it must be appreciated that terminal area incidents/accidents do not account for all of the incidents/accidents that occur.

TABLE A-I

NUMBER OF AIR CARRIER AIRCRAFT OPERATIONS[*] AT FAA FACILITIES[†]

YEAR		
1964	1965	1966
7,447,434	7,819,144	8,206,388

TABLE A-II

NUMBER OF AIR CARRIER INSTRUMENT APPROACHES[*]

YEAR		
1964	1965	1966
564,195	620,645	664,435

The data summarized here concerns only the takeoff and landing phases of flight as defined by the CAB.[*] The subphases of flight, as defined by the CAB, have been used to distinguish instrument flight incidents/accidents in the landing phase from the total of landing incidents/accidents. A similar approach cannot be applied to the takeoff data incidents/accidents because no means for distinguishing which arise during instrument flight exists. Furthermore, only those air carrier incidents/accidents are considered for which the aircraft involved has two or more engines, weighs more than 15,000 lb empty, has fixed wings; and which arise because of piloting difficulty, deficiency, or error; ATC deficiency or error; funda-mental aircraft or ground facility deficiency (such as navigation facility failure, improper runway maintenance, designed-in limitations, etc., which are primary for the takeoff/landing execution). However, mechanical/electrical/hydraulic failure induced incidents/accidents are not counted if

---

[*]Includes operations/instrument approaches by foreign air carriers and all nonfixed air carriers as well as by small and/or single-engine aircraft used in air carrier service.

[†]FAA Air Traffic Activity — Calendar Year 1966, Federal Aviation Agency, Office of Management Services, Jan. 1968.

● The resulting takeoff/landing is acceptable.

● The failure is beyond compensation by emergency piloting procedure, e.g., improper maintenance induced gear collapse on landing, even if an incident or accident occurs.

When improper implementation of emergency procedures is a heavily contributing cause to the incident/accident, it _is_ counted. This particularized view sometimes leads to interpretations of causes which deviate from those in the official FAA/CAB report on an incident/accident. This is necessary in order to represent accurately those terminal operations which are performance sensitive to the pilot-controller-display-aircraft-guidance system organization.

A statistical summary of accidents for the calendar years 1964 through 1966 constitutes Tables A-III and A-IV.

A similar statistical summary of incidents is also available. The need for incident statistics is twofold. By regarding incidents as "accidents wherein the deviation of the circumstances (variables) from nominal is not so large as to cause damage or injury," a broader data base and consequently higher confidence levels in the statistics are gained. This also provides a means for the generation of the very lowest probability events which, on the basis of accident data, would have to be approximated by guesstimate. Secondly, incident data produce an additional set of conditions by which the terminal operations model may be validated or constructed (but not both).

A statistical summary of terminal area aircraft incidents during 1964-1966 is included here as Table A-V. The availability of these incident statistics broadens the small base of data on deviations from desired flight conditions. However, it must be pointed out that these new data are generally not as reliable as the data concerning accidents. This is due to the lack of uniformity in reporting incidents. Each airline (and even different flight crews from the same airline) has its own point of view with regard to situations not severe enough to be considered accidents. In particular, less care is exercised in accurately recording the conditions leading to and surrounding an incident than would be the

A-3

TABLE A-III*

TYPES OF TERMINAL AREA ACCIDENTS AND THEIR STATISTICS

TYPE	SUBPHASE	OCCURRENCE PROBABILITY × 10^7 (TYPE ACC./TAKEOFF)	NO. IN YEARS			
			1964-1966	1964	1965	1966
TYPES OF TAKEOFF ACCIDENTS†						
Premature lift-off — stall — low airspeed	Roll, initial climb	5.112	6	3	3	0
Ground loop — aborted takeoff	Roll, aborted takeoff	3.408	4	0	0	4
Deviation from prescribed course	Initial climb	0.852	1	1	0	0
Evasive maneuver	Initial climb	0	0	0	0	0
Dragged wingtip	Roll, aborted takeoff	0	0	0	0	0
TYPES OF LANDING ACCIDENTS†						
Inadvertent gear retraction/failure to extend	Final approach, roll	5.112	6	3	1	2
Overshoot — ground loop Hydroplaning factor	Roll, level off/touchdown Roll	12.78/16.32*	15/3 (4/2)	5/3 (2/2)	4/0 (2/0)	6/0 (0/0)
Undershoot	Final approach (IFR or VFR)	16.19/27.03	19/5	7/2	7/3	5/0
Hard landing	Level off/touchdown	10.22	12	2	3	7
Line-up — swerve off runway	Final app., level off/touchdown	1.704/5.40	2/1	2/1	0/0	0/0
Dragged wingtip	Level off/touchdown, roll	0.852	1	0	1	0
Ground facility unsafe or failed	Initial approach (IFR or VFR), final approach, level off/touchdown, roll	1.704/0	2/0	1/0	1/0	0/0
Evasive maneuver	Initial approach (IFR or VFR), final approach (IFR)	0/0	0/0	0/0	0/0	0/0

* A Statistical Review and Resume of U. S. Air Carrier Accidents — Calendar Year 1964, Civil Aeronautics Board, Bureau of Safety, Safety Analysis Division, Sept. 1966.

A Statistical Review and Briefs of U. S. Air Carrier Accidents — Calendar Year 1965, Civil Aeronautics Board, Bureau of Safety, Analysis Division, Mar. 1967.

Annual Review — U. S. Air Carrier Accidents — Calendar Year 1966, National Transportation Safety Board, Dept. of Transportation, Dec. 1967.

† Includes U. S. Air Carrier accidents occuring in the 50 states, possessions, and protectorates.

* When two numbers appear, the first number is the total number of accidents of given type for visual and instrument flight; the second number is for those accidents which arise from instrument flight.

TABLE A-IV

OVERALL SUMMARY OF TERMINAL ACCIDENTS

TYPE OF OPERATION	OCCURRENCE PROBABILITY X 10^7	NO. OF ACCIDENTS 1964-1966
Takeoff	9.372 (Takeoff Acc./Takeoff)	11
Landing (total)	48.57 (Landing Acc./Landing)	57
(instrument flight)	48.67 (Inst. Land. Acc./Inst. App.)	9
Terminal	28.97 (Accidents/Operation)	68

case for an accident. Although this does not nullify the incident data, it does mean that fine grain details based on incident reports should not be used "to build a story around."

In addition to the gross numbers given in Table A-V (and the earlier tables) we also have a breakdown of the accidents and incidents by aircraft type. This data is presented in Table A-VI. The purpose for obtaining this information is to be able to particularize the system model to any given aircraft type, and have data to help in checking any differences predicted between aircraft.

It is noted that the relatively large number of landing accidents and incidents shown in Table A-VI for the B-727 is due, in part, to the newness of the airplane (during 1964-1966). In other words, an asymptotic level had not been reached on the learning curve for this airplane. That the DC-9 does not show such a large number of accidents/incidents is probably due to the small number of aircraft that were in operation during the years of interest (compared to the number of 727s).

TABLE A-V

TYPES OF TERMINAL AREA INCIDENTS AND THEIR STATISTICS*

	TYPE OF INCIDENT	SUBPHASE OF FLIGHT	OCCURRENCE PROBABILITY x 10^7	NUMBER IN YEARS			
				1964-1966	1964	1965	1966
TAKEOFF			(TYPE INC./TAKEOFF)				
	Premature lift-off, stall, low airspeed	Roll, initial climb	2.556	3	0	0	3
	Ground loop, aborted takeoff	Roll, aborted takeoff	16.189	19	1	3	15
	Deviation from prescribed course	Initial climb	1.704	2	0	0	2
	Evasive maneuver	Initial climb, roll	5.112	6	3	3	0
	Dragged wing tip, swerve	Roll, aborted takeoff	11.077	13	1	5	7
	Ground system failure	Roll, initial climb	0.852	1	0	1	0
APPROACH, LANDING			(TYPE INC./LANDING)				
	Inadvertent gear retraction/failure to extend	Final approach, roll	1.704	2	1	0	1
	Overshoot, ground loop	Roll, level off/touchdown	17.041	20	7	5	8
	Undershoot	Final approach	15.337	18	3	8	7
	Hard landing	Level off/touchdown	15.337	18	2	3	13
	Line up, swerve off runway	Final approach, level off/touchdown	49.419	58	16	19	23
	Dragged wing tip	Level off/touchdown, roll	14.485	17	1	4	12
	Ground facility/system unsafe, failed	Initial approach, final approach, level off/touchdown, roll	7.668	9	0	7	2
	Evasive maneuver	Initial approach, final approach	1.704	2	1	0	1

*These data have been summarized from public records made available through the Flight Standards Division of the FAA.
The data have been culled from the public records and classified according to the ground rules discussed in the 10 Oct. 1968
Quarterly Progress Report. In particular, incidents involving equipment failures only are generally excluded from consideration.

TABLE A-VI

TERMINAL AREA ACCIDENTS AND INCIDENTS BY TYPE OF AIRCRAFT FOR 1964-1966

TYPE AIRCRAFT	ACCIDENTS — TAKEOFF							ACCIDENTS — LANDING							INCIDENTS — TAKEOFF							INCIDENTS — LANDING						
	Premature lift-off, stall, low airspeed	Ground loop, aborted takeoff	Deviation from prescribed course	Evasive maneuver	Dragged wing tip, swerve	Ground facility failure or error	Inadvertent gear retraction, failure to extend gear	Overshoot, ground loop	Undershoot	Hard landing	Line-up, swerve off runway	Dragged wing tip	Ground facility unsafe, failed, or error	Evasive maneuver	Premature lift-off, stall, low airspeed	Ground loop, aborted takeoff	Deviation from prescribed course	Evasive maneuver	Dragged wing tip, swerve	Ground facility failure or error	Inadvertent gear retraction, failure to extend gear	Overshoot, ground loop	Undershoot	Hard landing	Line-up, swerve off runway	Dragged wing tip	Ground facility unsafe, failed or error	Evasive maneuver
B-727									3				1		2	1			1			2	5		5	7		
B-720	1							2	2	4								2					1	2	3	3	2	
B-707		1							1							2		2						4	1	1	2	
DC-9	1				1			2	1	2		1				1		1				4	1		1		1	
DC-8							1		2										3			3	2	2	2		1	
DC-7									2													1	2		3			
DC-6	3	1								1	2														1			
DC-3	1						1	2			1					2								2	2			1
CV-990																									1			
CV-880																									1			
CV-600																												
CV-580							1		2																1			
CV-440								2	1			1				1		1	1						1		1	
CV-340																												
CV-240																								1	1			
M-404																												
M-202																						3	1	2	3			
L-188																1							2		2		1	
L-1049 (1649)								2								3									1			
Viscount (V-812, 810, 745, 700)																		1	1		1	1			6	4	1	1
CL-44																												
Argosy AW-650	1								3								1								1			
F-27																			2	1		2			1			
C-54								2											1					2	1	4	1	
C-46																												
Beech 18*																												
Grumman G-73		1																										
Grumman G-44																												
BAC 1-11																												

*Does not meet gross weight ground rule.

A-7

APPENDIX B

EXAMPLE AIRPLANE AND CONTROL SYSTEM CHARACTERISTICS

This appendix contains a brief description of the longitudinal and lateral characteristics of the example airplane and several alternative approach controllers. A detailed development of these controllers (based on guidance, control, and regulation requirements) is presented in Ref. 12.

The example airplane is a DC-8 defined by the landing approach configuration parameters given in Table B-I. For the purpose of demonstrating the use of the approach model, three automatic longitudinal systems, a manual longitudinal flight-director system, and an automatic lateral system were used in the example calculations.

TABLE B-I

DC-8 PARAMETERS FOR LANDING APPROACH CONFIGURATION

GEOMETRY AND INTERIAL PROPERTIES		LONGITUDINAL STABILITY AXES		LATERAL BODY AXES	
h (ft)	0	X_u (1/sec)	-0.0373	Y_v (1/sec)	-0.0887
M (—)	0.204	X_w (1/sec)	0.136	$Y_{\delta_a}^*$ (1/sec)	0
V_{T_O} (ft/sec)	228.	X_{δ_e} (ft/sec^2/rad)	0	$Y_{\delta_r}^*$ (1/sec)	0.031
γ_O (deg)	-2.8°	X_{δ_T} (ft/sec^2/%)	0.106	L_β (1/sec^2)	-1.40
q (lb/ft^2)	61.8	Z_u (1/sec)	-0.283	L_p (1/sec)	-1.04
S (ft^2)	2758.	Z_w (1/sec)	-0.750	L_r (1/sec)	0.474
b (ft)	142.4	$Z_{\dot{w}}$ (—)	0	L_{δ_a} (1/sec^2)	1.13
c (ft)	22.16	Z_{δ_e} (ft/sec^2/rad)	-9.25	L_{δ_r} (1/sec^2)	0.159
W (lb)	180,000.	Z_{δ_T} (ft/sec^2/%)	-0.00097	N_β (1/sec^2)	0.368
m (slugs)	5,580.	M_u (1/sec-ft)	0	N_p (1/sec)	-0.029
I_x (slug-ft^2)	3.2×10^6	M_w (1/sec-ft)	-0.00461	N_r (1/sec)	-0.257
I_y (slug-ft^2)	3.8×10^6	$M_{\dot{w}}$ (1/ft)	-0.00085	N_{δ_a} (1/sec^2)	0
I_z (slug-ft^2)	6.6×10^6	M_q (1/sec)	-0.594	N_{δ_r} (1/sec^2)	-0.368
I_{xz} (slug-ft^2)	0	M_{δ_e} (1/sec^2)	-0.923		
X_{CG} (% c)	25.2	M_{δ_T} (1/sec^2/%)	0.000623		
δ_{F_O} (deg)	50	M_α (1/sec^2)	-1.05		
α_O (deg)	0.62	$M_{\dot{\alpha}}$ (1/sec)	-0.1936		

The control equations and functions accomplished by the three automatic systems are given in Table B-II. The systems are arranged from "A" to "C" in order of decreasing complexity and capability with "A" also standing for "advanced" and "C" for "conventional." All of the systems can acquire and maintain position on a straight line glide slope beam with well-damped path mode responses. However, System C is not suitable for following higher order paths with zero steady-state error. The major distinction between Systems B and C is in the θ feedback, which is washed out at very low frequencies on System B and not at all on System C. The washout is intended to improve the w_g windproofing, the steady-state following of higher order paths, and to remove the effects of any steady-state θ biases. This is achieved at the expense of a slight amount of path damping and bandwidth. Consequently, the superiority of System B in w_g windproofing and steady-state operations may be offset, for other inputs, by its smaller bandwidth.

System A is representative of the elevator axis of an advanced controller, typical of the forthcoming generation of low level approach and automatic landing systems. Appropriate feedbacks exist for all the functions listed for longitudinal control in Table B-II.

All of the example systems can be improved by the addition of an airspeed control. However, as they now stand without such a control, the speed variations of the three systems are nearly identical. Further, this similarity would not be changed if the same airspeed controller were added to all systems. Consequently, for the sake of simplicity, we have not provided airspeed control loops.

Block diagrams corresponding to the control equations in Table B-II are given in Figs. B-1 and B-2 for Systems A and C. A block diagram for System B would be essentially the same as that in Fig. B-2, except that the attitude feedback, K_θ, would be replaced by the transfer function, $K_\theta T_{wo} s / (T_{wo} s + 1)$.

An analysis of a manual control situation requires several considerations not found with automatic systems. One of these is the flight director mechanization. A block diagram for the longitudinal flight-director system is given in Fig. B-3, where it is seen that features from both Systems A and B

TABLE B-II

CONTROL EQUATIONS AND FUNCTIONS PERFORMED BY THE EXAMPLE AUTOMATIC LONGITUDINAL SYSTEMS

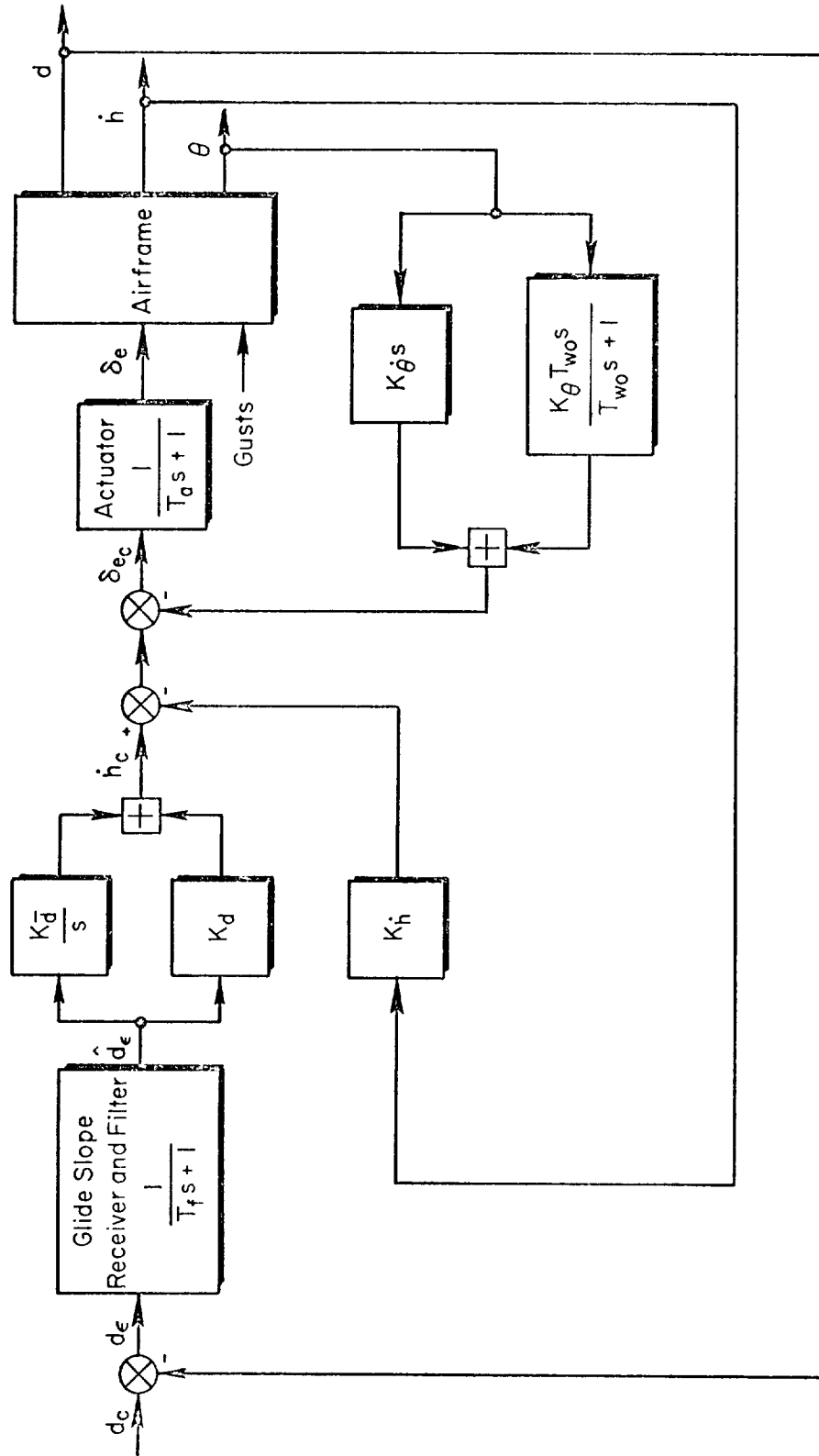|	FUNCTION	SYSTEM A	SYSTEM B	SYSTEM C
Attitude Control and Regulation	Short-Period Attitude Stiffness	$\theta \longrightarrow \delta_e$ in short-period frequency range		
	Short-Period Damping; Path Loop Bandwidth Extension Capability	$\dot\theta \longrightarrow \delta_e$ in short-period frequency range		
	Short Term w_g Windproofing	High-frequency θ washout	Low-frequency θ washout	No θ washout
Path Control and Regulation	Higher-order Path Following Trim Windproofing (w_g step)	$\int d\ dt \longrightarrow \delta_e$	Low-frequency θ washout	
	Path Acquisition and Stiffness Windproofing (u_g step, w_g pulse)		$d \longrightarrow \delta_e$	
	Path Damping	$\dot h \longrightarrow \delta_e$	$\theta \longrightarrow \delta_e$ in long-period frequency range	$\theta \longrightarrow \delta_e$
	Control Equations	$-\delta e_c = \dfrac{K_d + K_{\dot d}s}{s(T_f s + 1)}\, d_\epsilon + K_{\dot h}\dot h$ $\qquad + \dfrac{K_\theta s}{s + 1/T_{W2}}\,\theta + K_{\dot\theta}\dot\theta$	$-\delta e_c = \dfrac{K_d\, d_\epsilon}{T_f s + 1} + \dfrac{K_\theta s}{s + 1/T_{W1}}\,\theta$	$-\delta e_c = \dfrac{K_d\, d_\epsilon}{T_f s + 1} + K_\theta\,\theta$

Figure B-1. Block Diagram of Advanced Longitudinal Approach Control System [A]
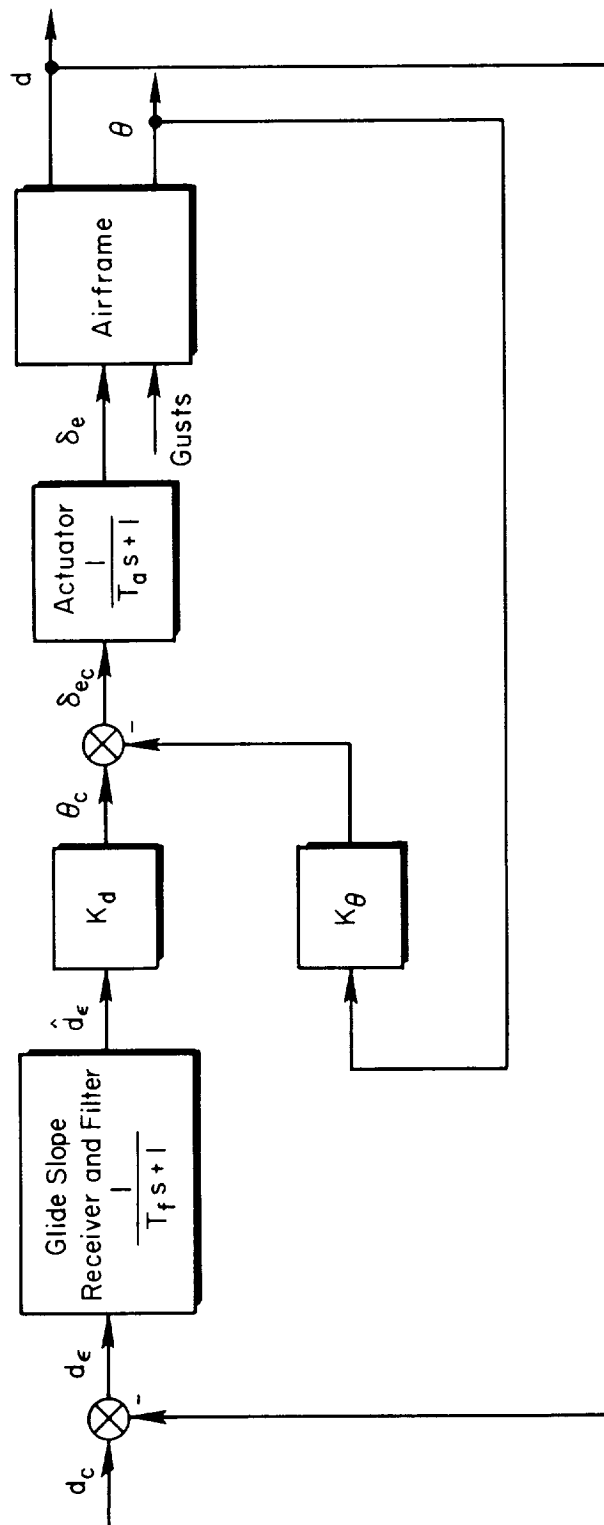
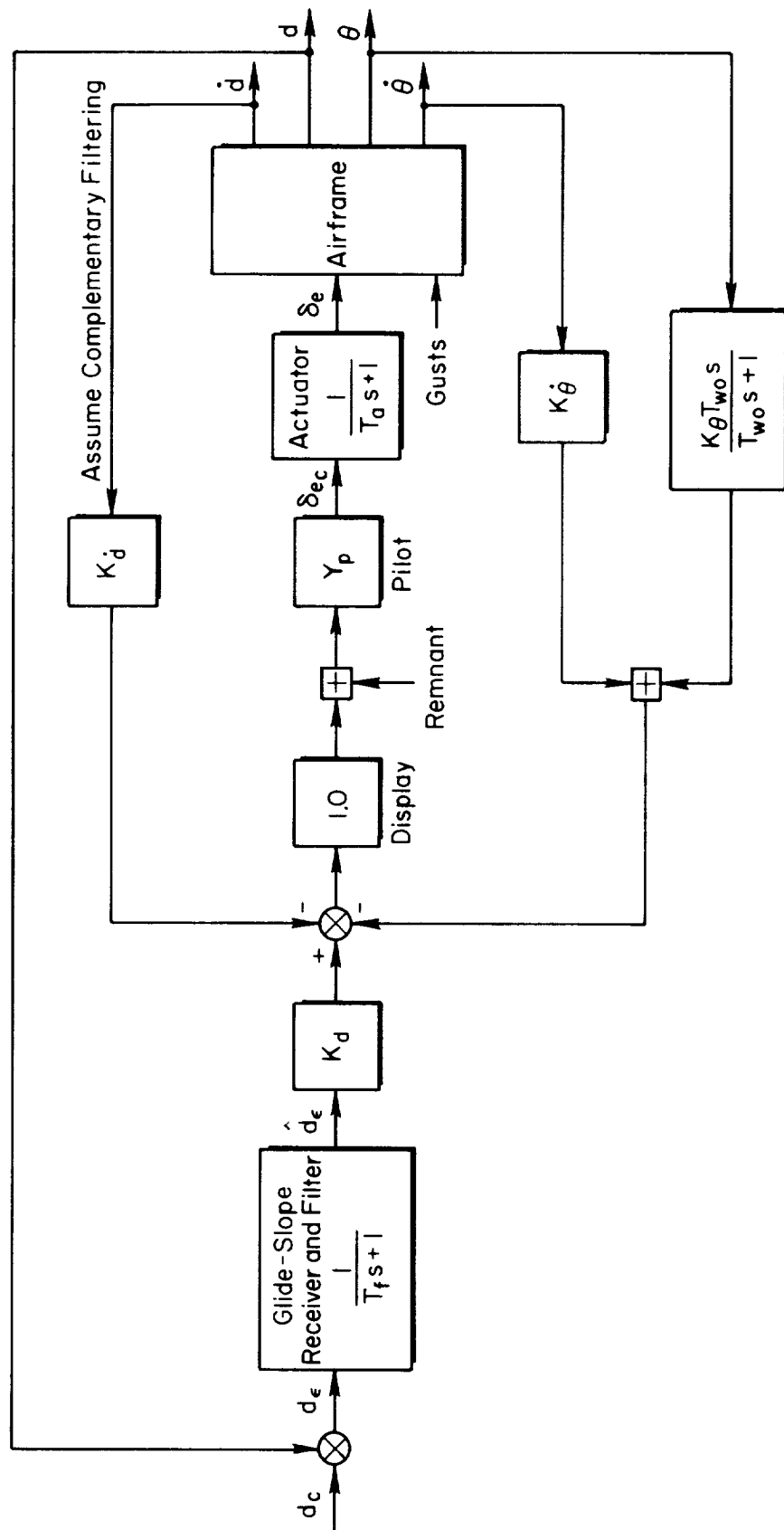Figure B-2. Block Diagram of Conventional Longitudinal Approach Control System [C]

Figure B-3. Block Diagram of Manually Controlled Longitudinal Flight Director System

are incorporated. This particular flight director represents an advanced flight director from Ref. 13.

Also required for a manual control situation are analytical descriptions of pilot behavior and pilot remnant. The estimated pilot describing function for the flight-director approach task is

$$Y_p = K_p\left(\frac{s+0.1}{s}\right)\left(\frac{10}{s+10}\right)e^{-0.35s} \qquad\qquad (B-1)$$

This form for the describing function is consistent with the results in Ref. 14, except for the integration, which was added to represent the pilot's behavior in nulling the flight-director command bars (as opposed to being content with a steady command bar offset). The magnitude of time delay (0.35 sec) is slightly larger than the values given in Ref. 14 for two basic reasons:

- The longitudinal flight-director tracking is not a full-attention task as was the case with the Ref. 14 experiments.

- Deviation of the manipulator from the ideal (heavily spring-restrained) will degrade the pilot's capabilities somewhat.

An estimate of the pilot remnant was based on data taken in DC-8 simulator experiments described in Ref. 10. It was assumed that the magnitude of the remnant scales with the displayed error (i.e., flight-director commands) such that the ratio of the correlated error power to the total error power is 0.8. This value of 0.8 was obtained from the reduced simulator data. No residual remnant was considered. The spectral shape of the estimated remnant is given by

$$\frac{\Phi_{nn_e}}{\sigma_e^2} = \left|\frac{K}{s+3}\right|^2 \qquad\qquad (B-2)$$

Knowing the mechanization of the flight director, and having estimates for the human pilot describing function and remnant allows the manual system to be analyzed in the same manner as automatic systems.

Table B-III summarizes the numerical values of the gains, time constants, etc., for each of the longitudinal example control systems.

TABLE B-III

SUMMARY OF NUMERICAL VALUES DEFINING THE
LONGITUDINAL EXAMPLE CONTROL SYSTEMS

SYSTEM	A	B	C	FLIGHT DIRECTOR	UNITS
K_θ	−2.0	−3.652	−3.652	−0.615	
$K_{\dot\theta}$	−2.0	0	0	−0.615	sec
$K_{\dot d}$ or $K_{\dot h}$	−0.0256	0	0	−0.00678	$\dfrac{rad}{ft/sec}$
K_d	−0.00867	−0.00514	−0.00514	−0.001356	$\dfrac{rad}{ft}$
$K_{\bar d}$	−0.000768	0	0	0	$\dfrac{rad}{ft\text{-}sec}$
$\dfrac{1}{T_{wo}}$	0.7	0.08	0	0.7	sec^{-1}
$\dfrac{1}{T_a}$	15.0	15.0	15.0	15.0	sec^{-1}
$\dfrac{1}{T_f}$	2.0	2.0	2.0	2.0	sec^{-1}
K_p	—	—	—	—	—

The automatic lateral control system used in the example calculations is defined in the block diagram of Fig. B-4. As with the longitudinal systems, guidance, control, and regulation requirements were the primary considerations that went into the development of the lateral system.
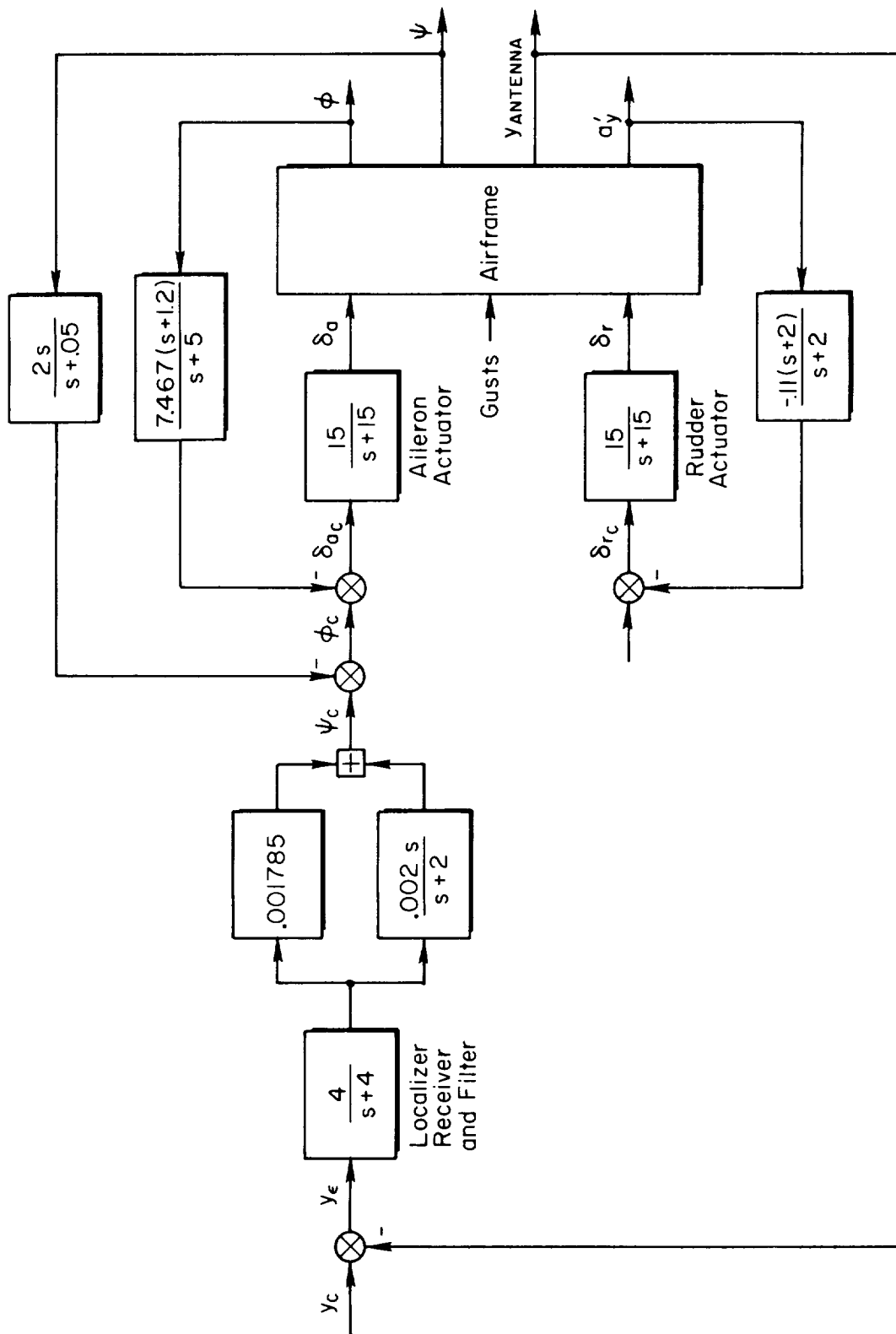
Figure B-1. Block Diagram of Lateral Approach Control System